Nanophotonics I: quantum theory of microcavities

Paul Eastham

http://www.tcd.ie/Physics/People/Paul.Eastham/

Contents

Introduction

What is nanophotonics?

Photonics is part of the modern science of light primarily concerned with the control, generation, and manipulation of optical signals. The wave lengths of this light are usually on the order of 1 μm = 1000 nm, so at first sight the relevance of nanoscale physics might appear strained. Nonetheless, it plays an essential role. This is because the goals of photonics require the light to be coupled to matter, and with this second component we must work on the nanoscale. We generate light from things like sodium atoms in a streetlamp, or an electron-hole plasma in a diode laser; steer and trap it with metallic or dielectric mirrors and waveguides – and then send it around the world with combinations of the two.

While the first laser exploited the natural atomic structure of a ruby crystal, we now engineer artificial atomic structures for use in optical systems. Arguably, nanophotonics is about the optical properties of these engineered structures, which include quantum dots, wells, and metallic nanocrystals. Because they derive from both the wave-like properties of light and the strong interactions within matter these optical properties are a significant challenge for theoretical physics.

As well as considering the effects of nanoscale matter on the propagation of light, a second aspect of nanophotonics is the trapping and manipulation of light on the scale of its wavelength. This comes in because there is so little of a nanoscale object, such as a quantum dot, that its effect on the entire electromagentic field is very small. However, if we introduce an optical cavity we create resonant modes of the electromagnetic field, which are localized in the cavity. For a smaller and smaller cavity, these resonant modes couple more and more strongly to a single nanoscale object inside it. Thus a single nanoscale object can have a noticeable affect on the electromagnetic field in a small cavity. One can then further increase the coupling by putting many nanoscale objects in the cavity. This direction, however, makes the system more linear, and therefore perhaps eliminates some interesting physical phenomena. The richest regime will probably turn out to be the intermediate one: a few, or few hundred, nanoscale objects in a microscale cavity.

Course overview

The aim of this course is to provide an introduction to some of the theoretical tools used to model solid-state light-matter systems. To do this, we will focus primarily on an important example: the semiconductor microcavity. By the end of the course, you should be able to construct theoretical models of some microcavities, and solve them to understand some of their simpler predictions. The vast majority of the remaining consequences of these theories are research problems.

Our aim in the first two chapters of the course is to understand how to construct a microcavity. This is a problem in classical optics and electromagnetism, which has both practical importance and interesting links to wave mechanics. Having done this, we shall then develop a quantum theory of the light trapped in microcavities (Chapter 3, 4), and combine this with the quantum theory of nanoscale objects in the microcavity (Chapter 5, 6). Chapter 5 considers the simplest case of a single atomic-like system in a cavity, while chapter 6 addresses the generalization to an ensemble of such systems, allowing us to treat the formation of polaritons in planar microcavities.

Although we develop a full quantum treatment of both light and matter, it may be worth noting that this full treatment is not always needed. Many of the effects known at present in microcavities can be described by treating the light as a classical wave, and reserving the quantum description to the matter. In this course we will approach from the fundamental quantum theory, and only then discuss the connection to the classical limit. This approach is hopefully accessible.

Problems

There are problems interspersed throughout these notes, some of which I will set as homework for assessment. These may well be questions which we have discussed during the lectures, but you are nonetheless expected to hand in written solutions. Questions marked ♠ are rather challenging, only for the keen, and will not be obligatory for assessment.

Chapter 1

Microcavity Electrodynamics

A microcavity[1, 2] is a structure designed to create resonant modes of the electromagnetic field, essentially by reflecting light so that it forms standing waves. The simplest toy model of such structure is a pair of high-reflectivity parallel mirrors, with some separation d, containing a material of refractive index n. For most incident frequencies the high mirror reflectivity means that incident light is strongly reflected. However, at the *resonant* frequencies the different reflections add up destructively. Thus the external reflectivity is very small and the light is transmitted through the structure (Fig. 1.1, left). This effect is caused by the presence of quasi-localized standing-wave modes of the electromagnetic field, which are optical analogs of the bound states of electrons in a potential well (Fig. 1.1, right).

The simplest treatment of this effect[3] is to calculate the reflected am-

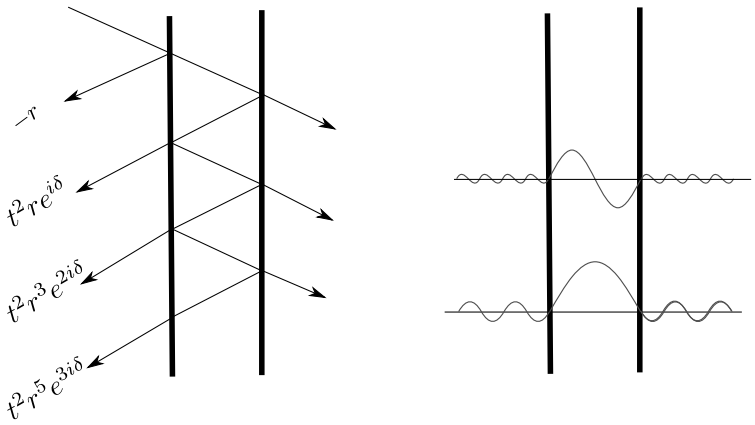

Figure 1.1: Left: The reflected amplitude from a double-mirror structure, where each mirror has amplitude reflectivity r and transmission t, can be calculated as shown. Right: The electric field profiles for scattering at the first two resonant frequencies show the connection to formation of standing wave modes between the mirrors.

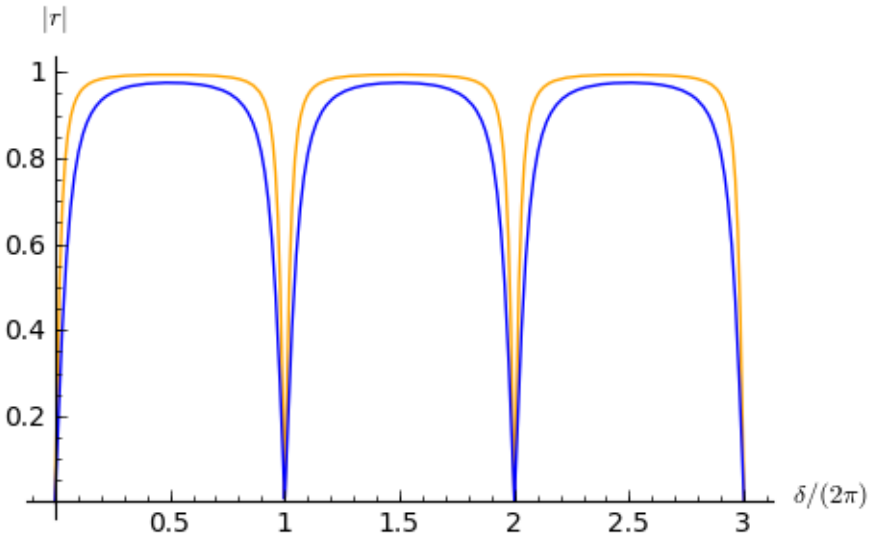

Figure 1.2: Calculated amplitude reflectivity $|r|$ for the structure in Fig. 1.1 with $r = 0.8$ (blue), $r = 0.9$ (orange).

plitude from the double-mirror structure shown in Fig. 1.1, in terms of the reflection and transmission coefficients of the mirrors. This is the sum over all the bounces

$$R = -r + \frac{t^2}{r}(r^2 e^{i\delta} + r^4 e^{2i\delta} + \ldots.) \tag{1.1}$$

$$= r\left(\frac{1-r^2}{e^{-i\delta} - r^2} - 1\right). \tag{1.2}$$

Here we have assumed lossless mirrors, for which $|r|^2 + |t|^2 = 1$. Fig. 1.2 shows when $r \approx 1$ we obtain the sharp resonant dips in the reflectivity. In fact, for lossless mirrors the reflectivity *vanishes* at the resonance condition $\delta = 2n\pi$. This is a surprising result: no matter how good the mirrors, they are effectively transparent at the resonance condition. If there are losses, e.g. due to the finite conductivity of metallic mirrors, $|r|^2 + |t|^2 < 1$, and the reflectivity dips but does not go to zero.

Because the reflectivity of the mirrors is finite, a standing wave mode of the cavity decays. Its finite lifetime, or finite damping, corresponds to the finite width of the resonances visible in Fig. 1.2. This effect is usually parametrized by the Q-factor of the resonator

$$Q = \frac{\omega_c}{\delta\omega}, \tag{1.3}$$

where $\delta\omega$ is the full-width at half-maximum of the resonance (in frequency). It measures the rate at which energy in the resonator decays, in this case due to the escape of photons through the mirrors.

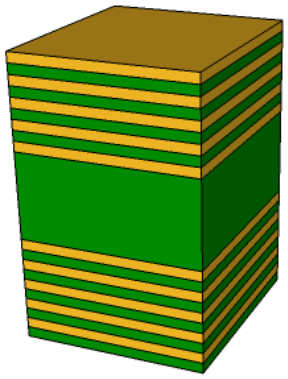

Figure 1.3: Schematic of a planar semiconductor microcavity with distributed Bragg reflectors. This is a planar semiconductor heterostructure, formed for example from layers of $Al_xGa_{1-x}As$ with different dopings x (colours). The variation in x gives layers of different refractive index, and hence reflections at the interfaces. These reflections create standing-wave modes of the electromagnetic field. Typically the "gap" layer has thickness $3\lambda/2$, while the repeating layers in the mirrors have thickness $\lambda/4$.

Question 1.1: Consider a driven harmonic oscillator with damping constant γ,

$$\ddot{x} + \gamma\dot{x} + \omega_0^2 x = Ae^{i\omega t}. \tag{1.4}$$

Write down the solution for $x(t)$ long after any transients have died away. Calculate and sketch the scaled square of the amplitude of the driven oscillations $f(\omega) = |x(t)|^2/A^2$. Calculate the width $\delta\omega$ of the response curve $f(\omega)$ in terms of the oscillator parameters. Show how the Q-factor $\omega_0/\delta\omega$ is related to the decay time for free (unforced) oscillations. (Assume $\gamma, (\omega - \omega_0) \ll \omega, \omega_0$)

It is relatively easy to make a high-Q resonator which is large, but it is much harder to make a wavelength-sized resonator for light. Our aim in the remainder of the first two lectures will be to understand how this can be done using semiconductor heterostructures. We focus on one such structure, the planar semiconductor microcavity with distributed Bragg reflectors (Fig.1.3). To understand the physics of this structure, we will first review the necessary aspects of classical electromagnetism. We will then see how to calculate the reflection and transmission of light incident on the simplest possible microcavity, formed from a layer of dielectric embedded in surroundings of a different refractive index. In the next lecture, we will see how *periodic* dielectric structures allow us to make much better mirrors, and hence useful microcavities. Along the way, we will further explore the connection between optical resonances and the bound states of quantum wells, described by the Schrödinger equation.

1.1 Revision of electromagnetism

The fundamental basis for both classical and quantum optics is Maxwell's equations in vacuum

$$\nabla \times \boldsymbol{B} = \mu_0 \boldsymbol{J} + \mu_0 \varepsilon_0 \dot{\boldsymbol{E}} \qquad \nabla \cdot \boldsymbol{E} = \rho/\varepsilon_0 \tag{1.5}$$

$$\nabla \cdot \boldsymbol{B} = 0 \qquad \nabla \times \boldsymbol{E} = -\dot{\boldsymbol{B}}. \tag{1.6}$$

In general one allows for the induced magnetic dipoles by introducing the magnetizing field $\boldsymbol{H}$ analogously to the electric displacement. However, in the following we are concerned with non-magnetic dielectrics, so can neglect this effect. $\boldsymbol{H}$ and $\boldsymbol{B}$ are then just be different names for the same thing, related by a universal constant $\boldsymbol{B} = \mu_0 \boldsymbol{H}$. See [4].

In matter, the electric and magnetic fields generally induce an electric polarization and magnetic moment. Most of these induced fields are proportional to the electromagnetic fields, so for the electric polarization we can write

$$\boldsymbol{P} = \epsilon_0 \chi \boldsymbol{E}, \tag{1.7}$$

which defines the susceptibility χ. We then define an "electric displacement" and relative permeability ϵ to include this polarization

$$\boldsymbol{D} = \epsilon_0 \boldsymbol{E} + \boldsymbol{P} = \epsilon_0 \epsilon \boldsymbol{E}, \tag{1.8}$$

$$\epsilon = 1 + \chi. \tag{1.9}$$

To the extent that Eq. (1.7) holds the material disappears from the problem, giving Maxwell's equations in a medium

$$\nabla \cdot \boldsymbol{D} = 0 \tag{1.10}$$

$$\nabla \cdot \boldsymbol{B} = 0 \tag{1.11}$$

$$\nabla \times \boldsymbol{H} = \dot{\boldsymbol{D}} \tag{1.12}$$

$$\nabla \times \boldsymbol{E} = -\dot{\boldsymbol{B}}. \tag{1.13}$$

Electromagnetic waves

From Eqs. (1.10–1.13) we find that the electric field in a uniform medium obeys the wave equation

$$\nabla^2 \boldsymbol{E} = \mu_0 \epsilon_0 \epsilon \ddot{\boldsymbol{E}}. \tag{1.14}$$

This has an infinite set of linearly-independent solutions, which are plane waves

$$\boldsymbol{E} = E^0_{\boldsymbol{e},\boldsymbol{k}} \boldsymbol{e} e^{i(\boldsymbol{k}.\boldsymbol{r} - \omega t)} \tag{1.15}$$

with phase velocity $v = \omega/|\boldsymbol{k}| = 1/\sqrt{\mu_0 \epsilon_0 \epsilon}$. The phase velocity differs from that of the vacuum via the refractive index n, $v = c/n$. A general solution is a superposition of these waves with different $\boldsymbol{k}, \boldsymbol{e}$,

$$\boldsymbol{E} = \sum_{\boldsymbol{e},\boldsymbol{k},\pm} E^0_{\pm,\boldsymbol{e},\boldsymbol{k}} e^{i(\boldsymbol{k}.\boldsymbol{r} - \omega t)}. \tag{1.16}$$

As usual, in a finite region of space there is a discrete set of allowed values of $\boldsymbol{k}$ which depend on the boundary conditions. The infinite system may be treated by introducing an artificial quantization volume $V \to \infty$. In the limit sums such as (1.16) become integrals involving a density-of-states (called the density-of-modes in the optics literature).

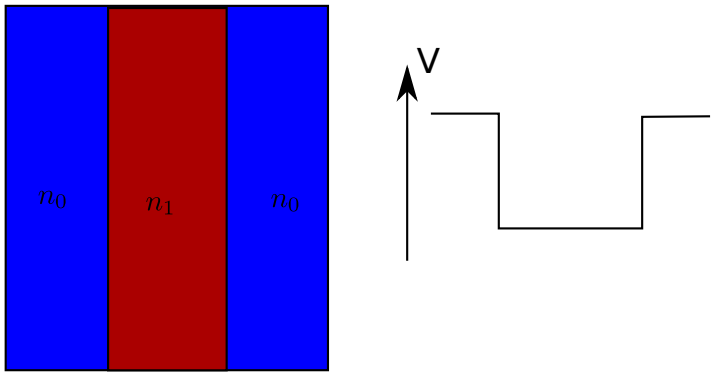

Figure 1.4: Simple microcavity consisting of a slab with refractive index n_1 embedded in a medium of index n_0. For $n_1 > n_0$ the wave equation for the electric field in such a dielectric corresponds to the Schrodinger equation for a particle in a potential well (right).

Polarization

As shown in question 1.2, the vectors $\boldsymbol{e}$ and $\boldsymbol{k}$ do not vary independently: generally $\boldsymbol{e}$ must be orthogonal to $\boldsymbol{k}$. We say that light is a transverse wave. For every $\boldsymbol{k}$ there are two linearly independent solutions, specified by a direction of $\boldsymbol{e}$. This degree-of-freedom is called the *polarization* of light[3]. A wave with a constant direction to $\boldsymbol{E}$ is called linearly polarized light. A superposition of two such solutions, identical apart from a $\pi/2$ phase shift and rotation of the direction of $\boldsymbol{E}$, is called circularly-polarized light. This is because the electric field vector rotates as the wave propagates.

Question 1.2: Show that only solutions of the wave equation with $\boldsymbol{e}$ and $\boldsymbol{k}$ perpendicular are solutions of Maxwell's equations.

Question 1.3: Show that, at a constant position, the direction of the electric-field vector in a circularly-polarized light wave rotates.

1.2 The wave equation in layered dielectrics

Microcavities are generally planar structures formed from media of varying refractive index, such as Fig. 1.4. We now develop a general formalism which allows us to calculate the optical properties of such a structure, effectively solving the wave equation in it.

The solution to (1.14) in a layered structure is determined by how the plane-wave solutions in each layer join up, i.e., the boundary conditions at the interfaces. Eqs. (1.12–1.13) require that the transverse components of $\boldsymbol{E}$ and $\boldsymbol{H}$ are continuous at the interfaces. This is a more complicated condition than you may be used to, for example when matching the wavefunctions in Schrödingers equation at a potential step. However, for

waves in which either $\boldsymbol{E}$ or $\boldsymbol{H}$ lies parallel to the interfaces, it is simple: $\boldsymbol{E}$ or $\boldsymbol{H}$ must be continuous across the interface. These are referred to as transverse-electric (TE) and transverse-magentic (TM) waves. TE and TM waves are "polarization eigenmodes" of planar dielectric structures: the interfaces preserve the polarization of such a wave. Problems involving arbitrarily-polarized wave can be treated by decomposing into the TE and TM eigenmodes. Thus one can describe, for example, the general change in polarization on reflection.

We focus on the case of a TE polarization, where the elementary solutions to (1.14) are of the form

$$\boldsymbol{E} = \boldsymbol{e}E(z)e^{i\boldsymbol{k}_\parallel\cdot\boldsymbol{r}_\parallel}e^{-i\omega t}, \tag{1.17}$$

and $E(z)$ obeys

$$-\frac{d^2E(z)}{dz^2} + \left[\frac{\omega^2}{c^2}(n_0^2 - n(z)^2) - \left(\frac{\omega^2 n_0^2}{c^2} - |\boldsymbol{k}_\parallel|^2\right)\right]E(z) = 0. \tag{1.18}$$

Adding and subtracting a background constant in this way shows clearly that the problem is equivalent[2, 3] to solving the one-dimensional Schrodinger equation

$$-\frac{\hbar^2}{2m}\frac{d^2\psi}{dz^2} + (V(z) - E)\psi = 0, \tag{1.19}$$

with the electric field envelope $E(z)$ playing the role of the wavefunction. As shown in Fig. 1.4, an upward step in refractive index corresponds to a downward step in the potential: potential wells map to layers of high refractive index.

Transfer matrices

To solve Eq. (1.18) in a general layered structure we use the transfer matrix technique[1]. The idea is to introduce an operation which "propagates the solution in space", i.e. takes the solution at one position z_0 and gives us the solution at another $z_1 > z_0$. Since (1.18) is second-order in space we actually need both $E(z_0)$ and $\frac{dE}{dz}|z_0$ to be able to do this, so we introduce the vector

$$\boldsymbol{\phi}(z_0) = \begin{pmatrix} E(z_0) \\ \frac{-i}{k_0}\frac{dE}{dz}|_{z=z_0} \end{pmatrix}. \tag{1.20}$$

The vacuum wavenumber $k_0 = \omega/c$ is included in the definition as it simplifies the notation later.

In more straightforward form, (1.18) is

$$\frac{d^2E(z)}{dz^2} = -(n^2k_0^2 - |\boldsymbol{k}_\parallel|^2)E(z) = -k_{z,n}^2E(z). \tag{1.21}$$

$k_{z,n} = k_0 n\cos\phi_n$ is the z-component of the wavevector in the medium with refractive index n, where ϕ_n is the angle to the normal in that medium.

Question 1.4: Can $k_{z,n}^2 < 0$? What happens?

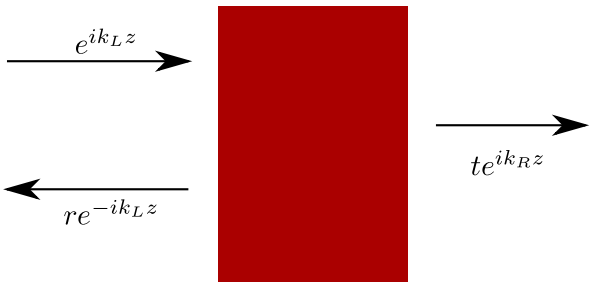

Figure 1.5: Scattering geometry used to calculate reflection and transmission coefficients from a 1D structure.

In each layer the solution is a sum of forward- and backward- propagating waves

$$E(z) = A^+ e^{ik_{z,n} z} + A^- e^{-ik_{z,n} z}. \tag{1.22}$$

Thus the transfer matrix which relates the fields at the left and right of a layer of thickness a must transform

$$\begin{pmatrix} A^+ + A^- \\ (k_{z,n}/k_0)(A^+ - A^-) \end{pmatrix} \rightarrow \begin{pmatrix} A^+ e^{ik_n a} + A^- e^{-ik_n a} \\ (k_{z,n}/k_0)(A^+ e^{ik_n a} - A^- e^{-ik_n a}). \end{pmatrix} \tag{1.23}$$

A little thought shows that it is

$$\boldsymbol{T}_{n,a} = \begin{pmatrix} \cos(k_{z,n} a) & i \sin(k_{z,n} a)/(k_{z,n}/k_0) \\ i(k_{z,n}/k_0) \sin(k_{z,n} a) & \cos(k_{z,n} a) \end{pmatrix}. \tag{1.24}$$

Since the boundary conditions are that $E(z)$ and $dE(z)/dz$ are continuous at the interfaces, it is clear that the transfer matrix across a boundary is just the identity matrix. Thus the transfer matrix for a layered structure is a product of that for the individual layers. For example, for the entire structure shown in Fig. 1.4 the fields on the right and left are related by

$$\phi|_R = \boldsymbol{T}_a \boldsymbol{T}_b \boldsymbol{T}_a \phi|_L. \tag{1.25}$$

Question 1.5: Show that the transfer matrix (1.24) produces the transformation (1.23).

Reflection and transmission coefficients

The usual practice in optics is to use transfer matrices to evaluate the reflection and transmission coefficients from the structure. This scattering geometry is shown in Fig. 1.5. We have

$$\boldsymbol{T} \begin{pmatrix} 1 + r \\ (k_{z,L}/k_0)(1 - r) \end{pmatrix} = \begin{pmatrix} t \\ (k_{z,R}/k_0) t \end{pmatrix}. \tag{1.26}$$

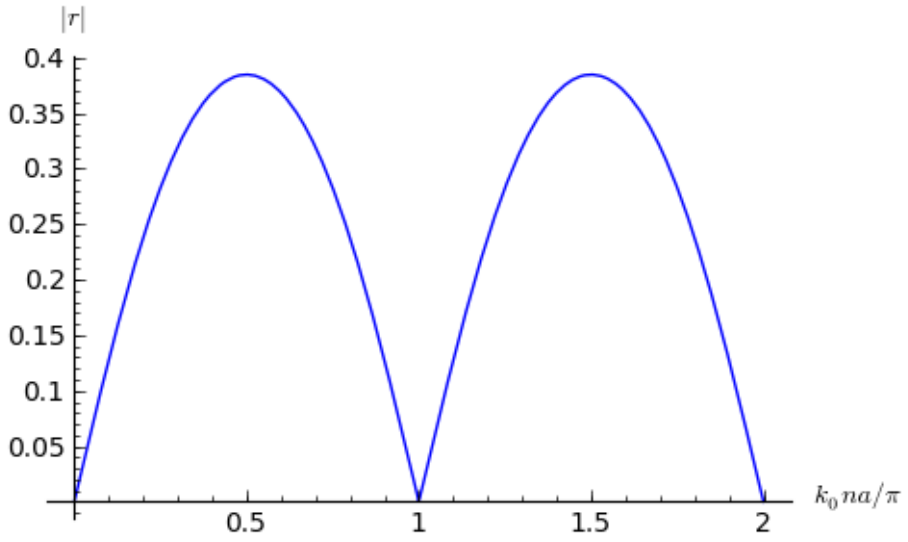

Figure 1.6: Reflectivity of a slab of dielectric with $n = 1.5$ of thickness a in air.

If we consider normal incidence $k_{z,n} = nk_0$, so

$$\boldsymbol{T}\begin{pmatrix} 1+r \\ n_L(1-r) \end{pmatrix} = \begin{pmatrix} t \\ n_R t \end{pmatrix}. \tag{1.27}$$

This equation can be solved to determine r and t as functions of the refractive indices and $k_0 = \omega_c$,

$$r = 1 + \frac{2n_R t_{11} - 2t_{21}}{n_R\left(-t_{11} + n_L t_{12}\right) + t_{21} - n_L t_{22}} \tag{1.28}$$

$$t = \frac{2n_L\left(t_{12}t_{21} - t_{11}t_{22}\right)}{n_R\left(-t_{11} + n_L t_{12}\right) + t_{21} - n_L t_{22}}. \tag{1.29}$$

Away from normal incidence, the z-component of the wavevector may be written $k_{z,n}/k_0 = n\cos\phi$, where ϕ is the angle to the normal in the medium. Thus the results away from normal incidence can be obtained by taking the normal-incidence expressions written in terms of the refractive indices, and substituting $n \to n\cos(\phi_n)$.

1.3 A planar resonator

To show the utility of the formalism, we can use it to calculate the reflection and transmission coefficients for a simple realistic structure: a slab of dielectric with $n = 1.5$ in air. The results are shown in Fig. 1.6. Notice that this is a very poor microcavity: the widths of the resonances are comparable with their separation, and $k_0 na \sim 1$, so Q is of order 1. In the next lecture, we shall see how to make microcavities with much better Q values.

Question 1.6: Suggest why the planar dielectric slab is such a poor microcavity.

1.4 Photonic eigenstates

To conclude this chapter, we try to connect the peaks in the reflection and transmission coefficients to the idea of eigenstates in Schrodinger's equation.

The usual practice in quantum mechanics is to find normalizable eigenstates of the wave equation. These are solutions which :

- Have a simple harmonic time dependence $\psi(z,t) \propto e^{i\omega t}$, and
- Satisfy the boundary conditions $\psi(z,t) \to 0$ as $z \to \pm\infty$.

Let us see where this procedure leads applied to the wave equation in a layered dielectric.

In terms of the transfer matrix, we have an eigenstate if the transfer matrix takes us from the boundary condition at the left to the boundary condition at the right – like waves fitting on a guitar string. Let us specifying boundary condition in terms of *outgoing* waves outside the structure. Thus the electric fields at the left boundary are of the form (1.22), with $A^- = 1, A^+ = 0$, and on the right with $A^+ = A, A^- = 0$. Since the transfer matrix connects the two sides, we have an eigenstate condition

$$\boldsymbol{T}\begin{pmatrix} 1 \\ -k_{z,L}/k_0 \end{pmatrix} = A\begin{pmatrix} 1 \\ k_{z,R}/k_0 \end{pmatrix}. \tag{1.30}$$

This gives a condition on the wavevectors of the outgoing waves – which is an implicit equation for the normal mode frequency, or eigenenergy:

$$t_{11}(k_{z,R}/k_0) - t_{12}(k_{z,L}/k_0)(k_{z,R}/k_0) + t_{22}(k_{z,L}/k_0) - t_{21} = 0, \tag{1.31}$$

or at normal incidence,

$$t_{11}n_R - t_{12}n_L n_R + t_{22}n_L - t_{21} = 0. \tag{1.32}$$

In general, (1.32) gives a *complex* n – really a complex $k_{z,n}$. To understand this, let us go back to the general expression

$$k_{z,n}^2 = n^2\omega^2/c^2 - |\boldsymbol{k}_\parallel|^2, \tag{1.33}$$

where $\boldsymbol{k}_\parallel$ is constant everywhere in the structure. Suppose first that $k_{z,n}$ is pure imaginary. Then there for any $|k_\parallel| > \Im(k_{z,n})$ there are solutions with real ω. These are *waveguide modes*, where light in the structure is totally internally reflected at the boundaries with the surroundings. Thus the fields outside are evanescent in the z direction, and there are real eigenmodes of the system analogous to the bound states of a quantum well.

The more general case of complex $k_{z,n}$ implies that ω is complex. This means that in the free evolution of the system the fields are decaying exponentials, i.e., there is a lifetime to the mode, and the system behaves like a *damped oscillator*. We know that when such a damped oscillator is driven it oscillates at the driving frequency, with an amplitude which depends on how close to resonance it is at. This is why any weakly damped photonic eigenmodes appear as sharp features in the reflection and transmission spectra: at those points we are driving a weakly damped oscillator

close to its resonant frequency, so the response becomes very large. This manifests itself as a reflection coefficient close to zero, and a transmission coefficient close to one.

This connection may be seen formally by noting that the same function of ω, $D(\omega)$ appears in the denominators of the expressions for the reflection and transmission coefficients and in the condition for a photonic eigenmode. Denoting the complex frequency by $z = \omega + I\gamma$, the eigenmode condition is $D(z) = 0$. Suppose now we have an eigenmode with a small γ. This means that there is a zero of $D(z)$ close to the real axis, so that $D(\omega)$ is small (roughly γ). Thus we see why close to ω there are sharp structures in the reflection and transmission coefficients. This is a general phenomenon in the scattering of waves from systems with bound or quasi-bound states. In quantum mechanics it is called *resonant tunneling*; for electrons, the effect is exploited in a device called a resonant tunneling diode. This electrical analog of the optical resonator consists of two tunnel barriers separated by a gap. Its electrical conductivity has sharp features as a function of bias voltage, which relate to the presence of quasi-bound states between the barriers.

1.5 Bibliography

[1] A. V. Kavokin, J. J. Baumberg, G. Malpuech, and F. P. Laussy, *Microcavities* (OUP, 2007).

[2] S. V. Gaponenko, *Introduction to Nanophotonics* (CUP, 2010).

[3] S. G. Lipson, H. Lipson, and D. S. Tannhauser, *Optical Physics* (CUP, 1995), 3rd ed.

[4] H. B. G. Casimir, Helv. Phys. Act. **41**, 741 (1968), reprinted in A random walk in science, IOP publishing 1973, p 71.

Chapter 2

Periodic optical structures and microcavities

In the last chapter, we saw how to solve the wave equation in planar dielectric structures. In this chapter, we apply these ideas to periodic planar dielectric structures. We shall then see how such structures allow us to make very good mirrors, and hence useful microcavities, which we shall discuss in the final part of the chapter.

2.1 Bloch theorem and photonic bandstructure

Suppose we have an infinite, periodic stack of dielectric layers, with period d. By Bloch's theorem the solution to Eq. (1.21) is of the form

$$E(z) = e^{iqz} U_E(z), \tag{2.1}$$

where $U_E(z)$ has period d. The vector $\boldsymbol{\phi}(z)$ defined by Eq. (1.20) behaves similarly,

$$\boldsymbol{\phi}(z) = e^{iqz} \boldsymbol{\Phi}(z), \tag{2.2}$$

where $\boldsymbol{\Phi}(z)$ is periodic. Thus we have

$$\boldsymbol{T}_d \boldsymbol{\Phi}(0) = e^{iqd} \boldsymbol{\Phi}(0), \tag{2.3}$$

where $\boldsymbol{T}_d$ is the transfer matrix connecting the fields across one period of the structure. Thus we see that e^{iqd} must be an eigenvalue of the matrix $\boldsymbol{T}_d$.

Because the transfer matrix preserves the normalization of the wave, $\det \boldsymbol{T}_d = 1$. The eigenvalue equation is then

$$\lambda^2 - \mathrm{Tr}(\boldsymbol{T}_d)\lambda + 1 = 0, \tag{2.4}$$

and writing $\lambda = e^{iqd}$ we have

$$2\cos(qd) = T_{11} + T_{22}. \tag{2.5}$$

This is a relationship between ω (remember $\boldsymbol{T}_d$ depends on frequency) and q, which is exactly analogous to the bandstructure of a one-dimensional

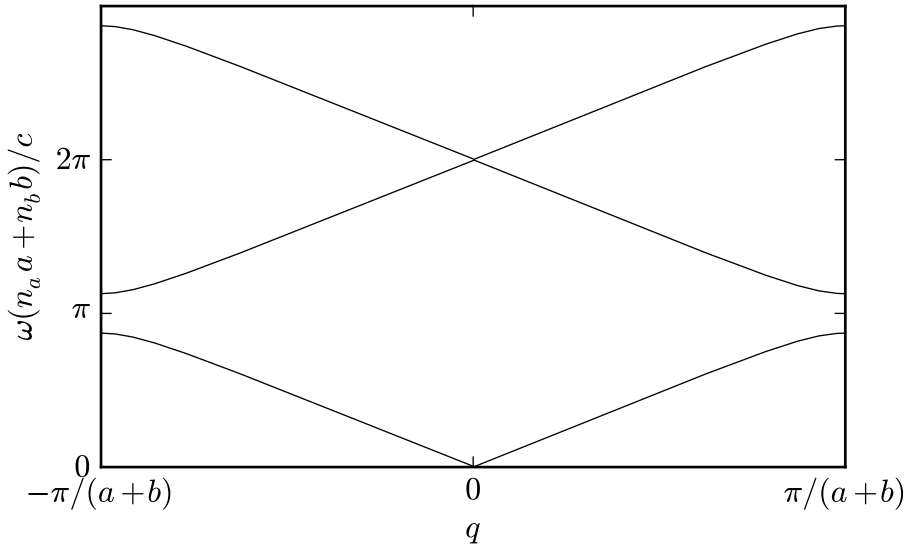

Figure 2.1: Photonic bandstructure for a periodic stack, with each period formed from two different layers of thickness a, b, and refractive indices n_a, n_b. $n_a a = n_b b$, $n_a = 1.5$, $n_b = 1$.

solid. It is therefore sometimes describes as a photonic bandstructure. An example is shown in Fig. 2.1, which shows the bandstructure for a repeating stack of two layers, with refractive indices n_a, n_b and thicknesses a, b.

A crucial feature of photonic bandstructures can be seen from (2.5): only if $|T_{11} + T_{22}| < 2$ do we have solutions. In general these solutions exist over ranges of frequencies called photonic bands. These are analogous to the electronic bands in solids. If this condition is not satisfied there are no solutions to the wave equation in the infinite periodic structure (the solutions with complex q are inadmissable as they do not satisfy Bloch's theorem). These regions of frequency correspond to the bandgaps in a solid, and are called stop-bands or photonic bandgaps. They can be seen along the vertical axis in Fig. 2.1.

It is worth emphasising that an evanescent wave (a complex q) cannot be a solution to the wave equation in a periodic system. An interpretation of evanescent solutions in the context of Bloch's theorem is wrong: in a periodic system these solutions simply do not exist. Evanescent solutions exist only at the boundaries of a periodic system, where Bloch's theorem does not apply.

2.2 Reflection from an infinite periodic structure

The extension of this theory to a semi-infinite medium [1], say in the region $z > 0$, does allow for solutions with complex q, and shows us how a periodic medium may be used to make a mirror. Consider reflection from the surface of a semi-infinite periodic medium. If we make the ansatz that the solution in the medium (say $z > 0$) is of the form (1.20), then the solution in the

medium has a q determined by solving (2.5) at the frequency of the incident beam ω. If ω lies in the stop-band the ansatz is solved for a complex q. Thus the field decays exponentially into the medium, i.e., is evanescent.

As one expects, if the field is evanescent in the medium, we have perfect reflection. To see this we note that in the stop bands the two eigenvalues of $\boldsymbol{T}_d$ are $\mu_1 = \lambda$, $\mu_2 = 1/\lambda$, with eigenvectors $\boldsymbol{e}_{12}$, and we may choose $|\lambda| < 1$. $\boldsymbol{e}_1$ then describes a decaying component, and $\boldsymbol{e}_2$ a growing one. Note from (2.2) that the decay length is $-d/\log|\lambda|$.

The incident field is

$$\phi(z=0) = \begin{pmatrix} 1+r \\ n_L(1-r) \end{pmatrix}. \tag{2.6}$$

Now notice that we must have

$$\phi(z=0) \propto \boldsymbol{e}_1 = \begin{pmatrix} a \\ ib \end{pmatrix} \tag{2.7}$$

if the field is not to grow indefinitely under the repeated action of the transfer matrix. It follows from the form of $\boldsymbol{T}_d$ that a, b are real in the stop band. Thus we have

$$r = \frac{n_L ia - b}{n_L ia + b} \tag{2.8}$$

$$\Rightarrow |r| = 1, \tag{2.9}$$

$$\arg r = \pi - 2\arctan\left(\frac{an_L}{b}\right). \tag{2.10}$$

Question 2.1: It is impossible to calculate a reflection cofficient from a semi-infinite medium outside the stop bands. Explain why. What does this mean for a large but finite structure? (Hint: think about generalizing the analysis above)

2.3 Properties of distributed Bragg reflectors

We have seen that a semi-infinite periodic stack creates, in general, perfect reflection over a set of frequency windows. Since the fields in the stop bands decay exponentially, it is clear that a stack much larger than the decay length $-d/\log|\lambda|$ will have a reflectivity close to one. Such mirrors are called distributed Bragg reflectors (DBRs).

The standard DBR consists of a periodic stack, in which each period has two layers a and b, with $n_a a = n_b b$. Henceforth we consider this case. As can be seen in Fig. 2.1, the centers of the stop-bands for such a stack appear at the frequencies

$$\omega(n_a a + n_b b)/c = \pi, 3\pi, 5\pi, \ldots. \tag{2.11}$$

This is (almost) the same as the Bragg interference condition in X-ray diffraction: bright spots (high reflectivity) appear when there is constructive interference between the reflections from successive periods of the structure. That is, the round-trip optical path length of the period should be a multiple of 2π:

$$2\omega(n_a a + n_b b)/c = 2\pi \times \text{integer}. \tag{2.12}$$

The fact that half of these are missing reflects the special choice $n_a a = n_b b$.

Question 2.2: Construct the transfer matrix $\boldsymbol{T}_d$ for one period of a distributed Bragg reflector with $n_a a = n_b b$ at normal incidence $\boldsymbol{k}_\parallel = 0$. Use Eq. 2.5 to derive expressions for the minimum, maximum, and center frequencies of the stop bands.

♠ Question 2.3: Compare plots of the right-hand side of Eq. 2.5 for a symmetric mirror, $n_a a = n_b b$, and an asymmetric one. Why might symmetric mirrors be preferable?

2.4 Microcavity

Since Bragg stacks make very good mirrors, we can use them to implement the double-mirror structure shown in Fig. 1.1. The ideal case is two identical semi-infinite Bragg stacks, separated by a defect layer of index n_c and size L. The frequencies of the bound states are determined by requiring that the round-trip phase is a multiple of 2π, i.e.,

$$\arg r(\omega) + \omega n_c L/c = \pi m. \tag{2.13}$$

In general $\arg r(\omega)$ varies with ω, as determined by (2.10). It is zero at the central frequency of the stop-band if the outermost layer of the mirror has the smaller refractive index, or π in the opposite arrangement. The spectrum is the same in either case, but in the first (second) the field profiles have antinodes (nodes) at the surface of the mirror. Fig. 1.1 shows the form of the field profile in the second case.

If the confined mode is not at the center frequency of the stop band then the mode frequency moves away from the naive value set by the mirror spacing L. This can be seen explicitly by noting that, provided we are not too close to the edge of the stop band, the phase change may be approximated as a linear function of ω, or $k_{z,0} = \omega/c$. Thus we can write the round-trip condition

$$\alpha(k_{z,0} - \bar{k}_{z,0}) + k_{z,0} n_c L = m\pi, \tag{2.14}$$

so

$$k_{z,0} = \frac{\pi m + \alpha \bar{k}_z}{\alpha + L n_c}, \tag{2.15}$$

in which the factor $L_{\text{eff}} = \alpha + L n_c$ appears as the effective confinement length. The parameter α is generally similar to the decay length of the mode through the Bragg mirror, which is usually much larger than L. Thus unless take care to design a structure where the resonance lies exactly in the centre of the stop band, the confinement energy will be controlled mostly by the decay into the mirrors rather than the cavity gap[2].

Real microcavities, such as Fig. 1.3, are simply truncated approximations to this ideal. The point is that the mirror reflectivity is so high that we can now produce optical cavities, on the scale of the wavelength, with very high Q factors. This can be seen in the reflection spectrum in Fig. 2.2.

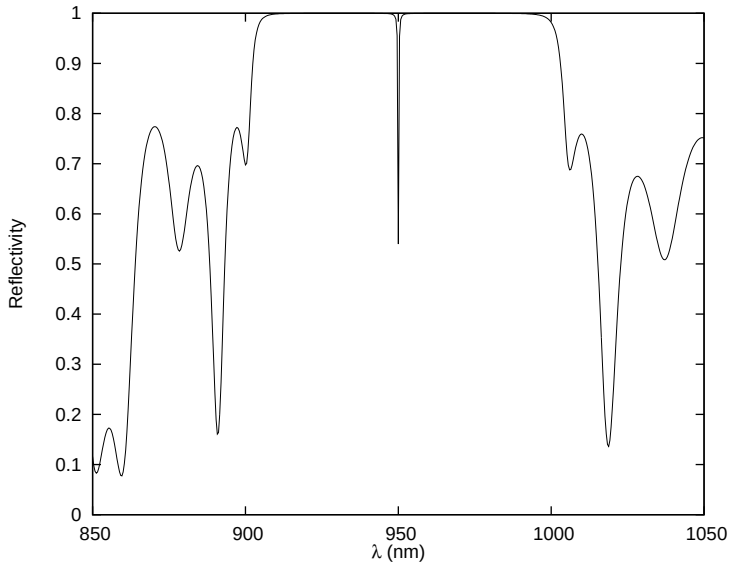

Figure 2.2: Calculated intensity reflectivity for a semiconductor microcavity structure at normal incidence. Note the very narrow peak in the middle of the stop band, which correspond to a long-lived confined resonant electromagnetic mode. Calculated by R. T. Phillips.

2.5 Dispersion relation in planar microcavities

An important feature of planar microcavities is their behaviour away from normal incidence. The transfer matrix across a layer of the DBR,

$$\boldsymbol{T}_a = \begin{pmatrix} \cos(k_{z,a}a) & i\sin(k_{z,a}a)/(k_{z,a}/k_0) \\ i(k_{z,a}/k_0)\sin(k_{z,a}a) & \cos(k_{z,a}a) \end{pmatrix}, \tag{2.16}$$

depends on the accumulated phase

$$k_{z,a}a = (\omega/c)n_a\cos\theta_a = (\omega/c)\bar{n}_a \tag{2.17}$$

as well as the frequency-independent factor

$$k_{z,a}/k_0 = n_a\cos\theta_a = \bar{n}_a, \tag{2.18}$$

which implements the changes in the reflection coefficients at the interfaces as we go to finite angles. Here θ_a is the angle of propagation to the normal in this layer of the mirror. The most important effect comes from the changes in the phase factors, so that the stop-band structures of the mirrors moves up to higher frequencies as we go to higher angles.

The same effect leads to a shift of the cavity resonances to higher frequencies with angle. So long as the axial wavevector $k_{z,n}$ is inside the stop-bands of the mirrors, its value at resonance is fixed by the round-trip condition [cf (2.13)]

$$\arg r(k_{z,n}) + k_{z,n}L = \pi m. \tag{2.19}$$

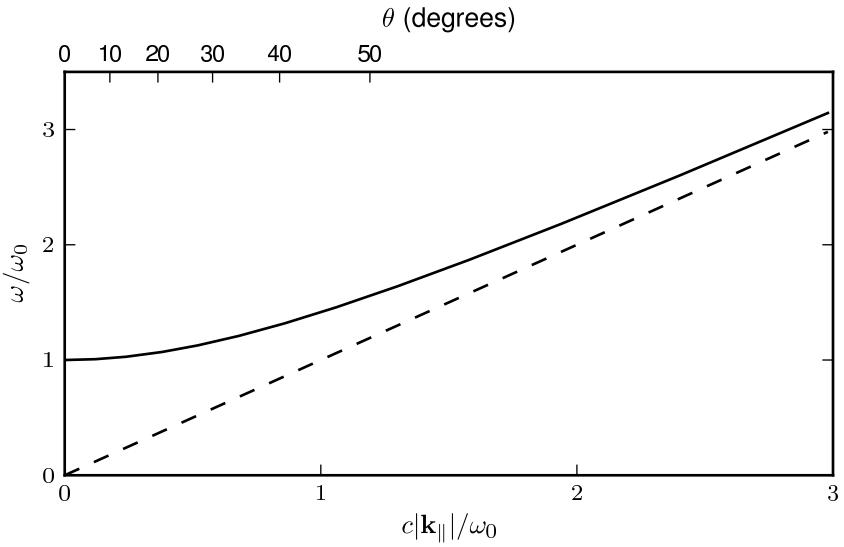

Figure 2.3: Dispersion relation for a confined mode in a planar cavity (solid line) and a photon in free space (dashed). The lower x axis is labelled with the in-plane wavevector. The upper is labelled with the angle of propagation to the cavity normal in vacuum.

The frequency where this resonance appears is

$$\omega^2 = (c^2/n^2)\left(k_{z,n}^2 + |\boldsymbol{k}_\parallel|^2\right) \tag{2.20}$$

$$= \omega_0^2 + (c^2/n^2)|\boldsymbol{k}_\parallel|^2. \tag{2.21}$$

$$\Rightarrow \omega \approx \omega_0 + \frac{c^2|\boldsymbol{k}_\parallel|^2}{2\omega_0}, \tag{2.22}$$

and the propagation direction outside the structure is of course $\tan^{-1}|\boldsymbol{k}_\parallel|/k_{z,0}$. This form for the dispersion relation is shown in Fig. 2.3. Notice that for small angles the dispersion relation $E = \hbar\omega$ is that of a non-relativistic massive particle in two dimensions, with effective mass $m = \hbar\omega_0/(c/n)^2$ and rest energy $\hbar\omega_0 = m(c/n)^2$ (this is not really a coincidence). Typically microcavities are designed so that ω_0 is an optical or near infrared frequency, say $\hbar\omega_0 = 1\text{eV}$, in which case $m \approx 10^{-6} m_{\text{el}}$.

2.6 Bibliography

[1] D. Felbacq, B. Guizal, and F. Zolla, Optics Communications **152**, 119 (1998), ISSN 0030-4018, DOI: 10.1016/S0030-4018(98)00134-5.

[2] M. S. Skolnick, T. A. Fisher, and D. M. Whittaker, Semiconductor Science and Technology **13**, 645 (1998).

Chapter 3

Quantum theory of light

In the quantum theory of a single particle, one learns that the particle position and momentum are operators, which obey the commutation rule

$$[\hat{q}, \hat{p}] = i\hbar. \tag{3.1}$$

The motion of the particle is governed by Schrödinger's equation

$$i\hbar \frac{\partial}{\partial t}|\psi\rangle = \hat{H}|\psi\rangle, \tag{3.2}$$

for the wavefunction $|\psi\rangle$. This is written in terms of the Hamiltonian operator

$$\hat{H} = \frac{\hat{p}^2}{2m} + V(\hat{q}). \tag{3.3}$$

Finally, one learns how to calculate the outcomes of experiments: these correspond to Hermitian operators $\hat{O}$, with complete sets of eigenvalues and eigenvectors λ_i, $|\lambda_i\rangle$. The outcome of an experiment on a system in state $|\psi\rangle$ is one of the eigenvalues, λ_j, with probability $|\langle\lambda_j|\psi\rangle|^2$. Immediately after a measurement yielding value λ_i, the state is $|\lambda_i\rangle$.

The foundations of the quantum theory of light are very similar to those of the quantum theory of a single particle. There are fundamental non-commuting quantities: the electric and magnetic fields. There is a wavefunction; a time evolution controlled by a Hamiltonian; and a measurement rule related to the non-commuting nature of the operators. The additional complexity appears because, whereas for a single particle there are two degrees of freedom – position and momentum – for the electromagnetic field there are an infinite number of degrees of freedom – the amplitude of the electric and magentic field at every point in space. You should already have seen theories like this: a simple example would be a set of harmonic oscillators

$$\hat{H} = \sum_i \frac{\hat{p}_i^2}{2m} + \frac{m\omega_i^2}{2}\hat{q}_i^2, \tag{3.4}$$

which you may recognise is the Einstein model of lattice vibrations in a solid.

To work effectively with quantum theories like (3.4), which are called quantum field theories, one needs a new set of bookeeping techniques: the language of second quantization. In this chapter we shall develop the quantum theory of light in, and alongside with, this new language. We shall see that this is the same theory one would write for a gas of bosons, an important general point:

Quantum field theory = Many particle physics,

or more specifically

Quantum electrodynamics = Many photon physics.

3.1 Quantum harmonic oscillator

The quantum dynamics of the electromagnetic field will turn out to be the same as that of (3.4). Let us first review the operator approach to solving the single harmonic oscillator. One defines the "annihilation operator"

$$\hat{a} = \sqrt{\frac{m\omega}{2\hbar}}\hat{q} + i\sqrt{\frac{1}{2\hbar m\omega}}\hat{p}, \tag{3.5}$$

and its Hermitian conjugate $\hat{a}^\dagger$. Notice that the prefactors involve the natural lengthscale, $\ell = \sqrt{\hbar/m\omega}$, and momentum scale, $m\omega\ell$, of the quantum harmonic oscillator, so that $\hat{a}$ is a dimensionless operator. The algebra of these operators is

$$[\hat{a}, \hat{a}^\dagger] = 1. \tag{3.6}$$

They allow us to write the harmonic oscillator Hamiltonian as

$$\hat{H} = \hbar\omega\left(\hat{a}^\dagger\hat{a} + \frac{1}{2}\right). \tag{3.7}$$

This quantity is basically the number operator $\hat{N} = \hat{a}^\dagger\hat{a}$. Because only energy differences are significant the final energy term can be dropped in many calculations, although there are situations in which it can and does have measurable effects.

We now notice that if $|n\rangle$ is an eigenstate of $\hat{N}$ with eigenvalue n, $\hat{a}|n\rangle$ is an eigenstate with eigenvalue $n-1$. In fact,

$$\hat{a}|n\rangle = \sqrt{n}|n-1\rangle. \tag{3.8}$$

Similarly, we find that

$$\hat{a}^\dagger|n\rangle = \sqrt{n+1}|n+1\rangle. \tag{3.9}$$

Since the operator $\hat{N} = \hat{a}^\dagger\hat{a}$ is positive-definite, there must be a state corresponding to the lowest eigenvalue. $\hat{a}$ must annihilate this state, i.e.

$$a|0\rangle = 0, \tag{3.10}$$

and so the eigenvalue of $\hat{N}$ for this state is zero.

It therefore follows that the eigenspectrum of $\hat{N}$ is the discrete ladder of states $|n\rangle$, where $n = 0, 1, 2, 3 \ldots$, with eigenvalues n of $\hat{a}^\dagger \hat{a}$. These states are called "Fock states" or "number states", and can all be constructed by repeated application of $\hat{a}^\dagger$ to the "vacuum state" $|0\rangle$. In more familiar terminology, this vacuum state $|0\rangle$ is the ground state of the harmonic oscillator.

Since we have shown how to construct all the eigenstates of the Hamiltonian – which form a complete set, since the Hamiltonian is a Hermitian operator – we can now solve any problem in the physics of the quantum Harmonic oscillator.

Question 3.1: Consider a harmonic oscillator prepared in the (unnormalized) state at $t = 0$, $|a(t = 0)\rangle = (\hat{a}^\dagger \hat{a}^\dagger + \hat{a}^\dagger)|0\rangle$. What are the outcomes of a measurement of the energy in this state, and with what probabilities?

Question 3.2: What is the expectation value of the position of the oscillator in question 3.1 at time t?

In problems involving harmonic oscillators one is often particularly interested in the position of the particle, for which it is useful to find the position-space wavefunctions $u_n(q) = \langle q|n\rangle$, where $|n\rangle$ is a Fock state and $|q\rangle$ an eigenstate of the position operator. A neat way to do this is to note that the ground state obeys

$$\hat{a}|0\rangle = 0. \tag{3.11}$$

In position space this reads

$$\frac{1}{\sqrt{2}}\left(\frac{q}{\ell} + \ell\frac{d}{dq}\right) u_0(q) = 0. \tag{3.12}$$

This equation can be solved to determine the ground-state wavefunction $u_0(q)$

$$u_0(q) = \left(\frac{1}{\pi}\right)^{1/4} \frac{1}{\sqrt{\ell}} e^{-q^2/2\ell^2}. \tag{3.13}$$

The remaining wavefunctions for the Fock states (energy eigenstates of the harmonic oscillator), can then be found by repeatedly applying the real-space form of the differential operator $\hat{a}^\dagger$ to this wavefunction.

Question 3.3: Sketch, or plot numerically, a function showing the possible outcomes of the measurement of q (x-axis), and their probability density (y-axis) in the Fock states $|0\rangle, |1\rangle$.

3.2 Heisenberg picture

In elementary quantum mechanics one normally works in what is called the Schrodinger picture or representation. In this representation the operators, which determine the observables of the system from the wavefunction, are

time-independent, while the wavefunction is time-dependent. In the following we shall sometimes need an alternative picture, in which we work with time-dependent operators and time-independent wavefunctions. This is known as the Heisenberg picture.

To make the transition to the Heisenberg picture, we note that the expectation value of an operator B is

$$\langle\psi(t)|B|\psi(t)\rangle. \tag{3.14}$$

The formal solution to the Schrodinger equation is

$$|\psi(t)\rangle = e^{-iHt/\hbar}|\psi(0)\rangle, \tag{3.15}$$

so the expectation value (3.14) can be rewritten as

$$\langle\psi(0)|e^{iHt/\hbar}Be^{-iHt/\hbar}|\psi(0)\rangle. \tag{3.16}$$

This defines the Heisenberg picture operator

$$B_H(t) = e^{iHt/\hbar}B_S e^{-iHt/\hbar}, \tag{3.17}$$

and wavefunction

$$|\psi\rangle_H = |\psi(t=0)\rangle_S. \tag{3.18}$$

All physical quantities are the same in the two pictures; it is merely a matter of preference whether one writes the time dependence in the wavefunctions or the operators. Differentiating (3.17), gives a useful operator equation for $B_H(t)$,

$$i\hbar\dot{B}_H(t) = [B_H(t), H], \tag{3.19}$$

which is called the Heisenberg equation.

Question 3.4: Repeat the calculation of question 3.2 in the Heisenberg picture.

3.3 Quantum theory of an electromagnetic cavity

To understand the formalism of quantum electrodynamics, let us focus on the case of x-polarized electromagnetic waves propagating along the z-axis of a planar conducting cavity as shown in Fig. 3.1. Thus we have $\boldsymbol{E}(\boldsymbol{r},t) = \boldsymbol{i}E_x(z,t)$. We suppose the cavity is a perfect conductor, for which the general boundary conditions are

$$\boldsymbol{n}\times\boldsymbol{E} = 0 \tag{3.20}$$

$$\boldsymbol{n}.\boldsymbol{B} = 0 \tag{3.21}$$

on the surfaces. In our case $E_x(z,t) = 0$ at $z = 0$ and $z = L$. We expand the field as

$$E_x(z,t) = \sum_n \sqrt{\frac{2\omega^2 m}{V\epsilon_0}}\sin(kz)q_n(t), \tag{3.22}$$

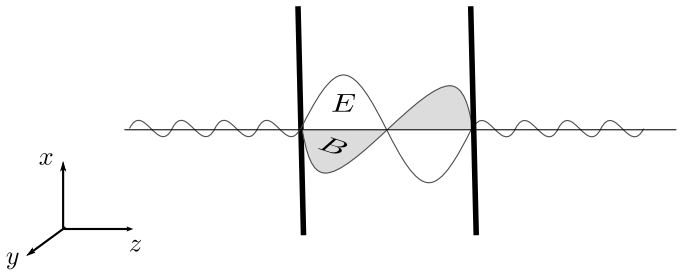

Figure 3.1: Single electromagnetic mode of a model one-dimensional cavity with conducting mirrors

where $k = n\pi/L$. The corresponding magnetic field B_y is

$$B_y(z,t) = \sum_n \frac{\epsilon\mu}{k}\sqrt{\frac{2\omega^2 m}{V\epsilon_0}}\cos(kz)\dot{q}_n(t). \tag{3.23}$$

The mass m in (3.22) defines a normalization of the mode coordinate $e_n(t)$ which is, in the classical theory, arbitrary. We use introduce a constant with units of mass so that $e_n(t)$ has the units of length, for reasons which will become apparent in a moment.

The important feature is that *any* allowed electromagnetic field in our problem can be decomposed as (3.22) and (3.23). The (related) functions in this decomposition are called the electric and magnetic mode functions; here they are proportional to $\boldsymbol{i}\sin(kz)$ and $\boldsymbol{j}\cos(kz)$.

Question 3.5: Use Maxwell's equations to show that (3.23) is the magnetic field corresponding to (3.22).

Now substitute the mode decomposition (3.22,3.23) into the energy for the electromagnetic field, we have

$$H = \frac{1}{2}\int d^3r \left(\epsilon_0|E_x|^2 + \mu_0|H_y|^2\right) \tag{3.24}$$

$$= \sum_n \frac{m\omega_n^2 q_n^2}{2} + \frac{m\dot{q}_n^2}{2} \tag{3.25}$$

$$= \sum_n \frac{m\omega_n^2 q_n^2}{2} + \frac{p_n^2}{2m}. \tag{3.26}$$

We identify this as the energy for a set of harmonic oscillators, one for each mode of the cavity, and each with mass m (so $p = m\dot{q}$). Similarly, this representation transforms the equations of motion – i.e. Maxwell's equations – into the equations for a set of independent harmonic oscillators. These oscillators are called "radiation oscillators".

Question 3.6: Derive (3.25) from (3.24).

The reason for pursuing this mode decomposition is that we know how to write a sensible quantum theory for a harmonic oscillator. Take the classical Hamiltonian, which is the energy written in terms of the position q and momentum p, and replace these quantities with operators obeying

$$[\hat{q}, \hat{p}] = i\hbar. \tag{3.27}$$

The result is the quantum Hamiltonian which controls the time-dependence of the system according to Schrodinger's equation. This rule is called "canonical quantization".

Following the canonical quantization rule, we obtain the quantum Hamiltonian for the electromagnetic field in the cavity, which is (3.26) with the operator substitution $p_n \to \hat{p_n}$, $q_n \to \hat{q_n}$. The operators obey the commutation rules

$$[\hat{q}_n, \hat{p}_n] = i\hbar\delta_{n,n'}. \tag{3.28}$$

As before, we make this theory tractable by rewriting it in terms of creation and annihilation operators

$$\hat{a}_n = \sqrt{\frac{m\omega}{2\hbar}}\hat{q_n} + i\sqrt{\frac{1}{2\hbar m\omega}}\hat{p}_n, \tag{3.29}$$

which obey $[\hat{a}_n, \hat{a}_n^\dagger] = 1$. Of course this gives

$$\hat{H} = \sum_n \hbar\omega_n \left(\hat{a}_n^\dagger \hat{a}_n + \frac{1}{2}\right). \tag{3.30}$$

More interesting is the form of the mode decompositions (3.22,3.23), which become the operators corresponding to the electric and magnetic fields

$$\hat{E}_x(z) = \sum_n \frac{\mathcal{E}_n}{\sqrt{2}}(a_n + a_n^\dagger)\sin(k_n z) \tag{3.31}$$

$$\hat{B}_y(z) = \sum_n \left(-\frac{i\mathcal{E}_n}{c\sqrt{2}}(a_n - a_n^\dagger)\right)\cos(k_n z). \tag{3.32}$$

The normalization constant

$$\mathcal{E}_n = \sqrt{\frac{2\hbar\omega_n}{V\epsilon_0}}, \tag{3.33}$$

is a fundamental unit of electric field, which appears in our system of units once we introduce $\hbar$. It corresponds to the harmonic oscillator length ℓ in the mechanical analogy. The quantity $\mathcal{E}_n/\sqrt{2}$ is the amplitude of the electric field associated with a photon.

The operators $\hat{E}_x(z), \hat{B}_y(z)$ do not commute – remember they are basically the position and momentum operators – so that in general there is an uncertainty relation between the electric and magnetic fields, and these fields are not simultaneously measurable with arbitrary precision. Nor do these operators commute with the Hamiltonian, so that in general we expect the results of measurements of the electric or magnetic fields to have quantum mechanical fluctuations.

3.4 Second quantization

Let us see what all this has to do with "photons", by considering an apparently different problem: the quantum mechanics of N non-interacting bosons in some potential. The Hamiltonian is

$$H = \sum_i \frac{\hat{p}_i^2}{2m_i} + V(\hat{q}_i). \tag{3.34}$$

The eigenfunctions of this Hamiltonian are products of the eigenfunctions for the one-particle problem, like

$$\phi_1(q_1)\phi_3(q_2)\phi_7(q_3)\ldots. \tag{3.35}$$

This particular function corresponds to a state where particle 1 is in energy level 1, 2 in energy level 3, and so on. However, we know that this is not a valid wavefunction for indistinguishable particles in quantum mechanics, because it violates the indistinguishability. Instead we should form the symmetrized (antisymmetrized) wavefunction for bosons (fermions)

$$\begin{aligned}\frac{1}{\sqrt{N_P}}(&\phi_1(q_1)\phi_3(q_2)\phi_7(q_3)\\ &\pm\phi_1(q_2)\phi_3(q_1)\phi_7(q_3)\\ &\pm\phi_1(q_1)\phi_3(q_3)\phi_7(q_2)\\ &+\ldots,\end{aligned} \tag{3.36}$$

where N_P is the number of permutations involved.

Writing out wavefunctions like (3.36) is tedious and pointless, because by the fact of indistinguishability we know that the only information in the wavefunction is the *number* of particles occupying each of the energy levels of the single-particle Hamiltonian. So one can write the wavefunction with only these labels,

$$|n_1, n_2, n_3, \ldots\rangle, \tag{3.37}$$

where the first slot in the ket denotes the number of particles in eigenstate 1, the second in eigenstate 2, and so on. These are the "N-particle Fock states". They form a complete basis in the space of wavefunctions of an N-particle system. Thus in describing an N particle system, one can work not with real-space wavefunctions like (3.36), but with the Fock states of a single-particle Hamiltonian. The single-particle Hamiltonian chosen does not even have to be related to the actual Hamiltonian although it generally helps if it is. The set of Fock states for all possible values of N forms a basis for describing the wavefunctions of any many-particle system of the right symmetry (bosons or fermions). Henceforth we shall focus on bosons.

To actually work with Fock states, one defines the operators

$$a_i|n_1, n_2, \ldots, n_i, \ldots\rangle = \sqrt{n_i}|n_1, n_2, \ldots, n_i - 1, \ldots\rangle. \tag{3.38}$$

$$a_i^\dagger|n_1, n_2, \ldots, n_i, \ldots\rangle = \sqrt{n_i + 1}|n_1, n_2, \ldots, n_i + 1, \ldots\rangle \tag{3.39}$$

These operators respectively annihilate and create a particle in the i^{th} single-particle state, and hence allow us to construct any Fock state systematically from the state with no particles, $|0\rangle$. The factors like $\sqrt{n_i}$ ensure that one cannot annihilate a particle which does not exist, and magically keep track of the correct normalization factor N_p in (3.36).

Any operator, such as the terms in the Hamiltonian, can be written in terms of the creation and annihilation operators. The form for a one-particle operator $\hat{O}$, like the non-interacting Hamiltonian (3.34), is

$$\sum_{ij} a_i^\dagger O_{ij} a_j, \tag{3.40}$$

where

$$O_{ij} = \int \phi_i^*(r) \hat{O} \phi_j(r) d^D r \tag{3.41}$$

is the matrix element of $\hat{O}$ between the single-particle basis states. For the Hamiltonian (3.34) of course, $H_{ij} = \delta_{ij} E_i$, so its second-quantized representation is

$$H = \sum_i E_i a_i^\dagger a_i. \tag{3.42}$$

It turns out that the operators a_i, a_j obey the commutation rules

$$[a_i, a_j] = 0 \quad [a_i, a_j^\dagger] = \delta_{ij}. \tag{3.43}$$

You can recognise these as identical to those for the creation and annihilation operators for the harmonic oscillator, and the electromagnetic field. Furthermore, the Hamiltonian (3.42) has exactly the same form as (3.30). Therefore :

- Quantum electrodynamics is mathematically identical to the quantum mechanics of a gas of non-interacting bosons, occupying energy levels corresponding to the classical normal modes of the electromagnetic field.
- These bosons are called photons.

Second quantization works almost identically for a system of fermions, such as electrons. The fermonic creation and annihilation operators for one orbital obey (3.38,3.39), but we must take

$$[c_i, c_j]_+ = [c_i, c_j^\dagger]_+ = 0, \tag{3.44}$$

for different orbitals i, j. Here $[A, B]_+$ is the anticommutator $AB + BA$. This definition, with the anticommutator, keeps track of the minus signs in (3.36). For coincident orbitals we find

$$[c_i, c_i^\dagger]_+ = 1, \tag{3.45}$$

so the commutation relations are analogous to (3.43) with anticommutators rather than commutators.

3.5 Free-space quantum electrodynamics

The procedure above can be followed generally, to determine the form of quantum electrodynamics in an arbitrary cavity, or even in free space. As a second, and important, example, let us see how this free-space quantization works. To do this we introduce a large cubic cavity of side L, and impose periodic boundary conditions on the faces. The appropriate electric mode functions are then the plane waves

$$\sqrt{\frac{\hbar\omega_k}{2\epsilon V}}\boldsymbol{\epsilon}e^{i\boldsymbol{k}.\boldsymbol{r}}. \tag{3.46}$$

The cavity requires $\boldsymbol{k} = 2\pi(n_x, n_y, n_z)/L$. Since we require $\boldsymbol{k}.\boldsymbol{\epsilon} = 0$ there are two independent values of the polarization vector $\boldsymbol{\epsilon}$ associated with each of these allowed electric field modes.

As before, Maxwell's equations reduce to an ensemble of independent harmonic oscillators, one for each of the modes, which we quantize to obtain the form (3.30). The normal modes are now specified by the wavevector $\boldsymbol{k}$ and polarization, and have frequency

$$\omega = c|\boldsymbol{k}|. \tag{3.47}$$

The electric and magnetic field operators take the forms

$$\boldsymbol{E}(\boldsymbol{r}) = \sum_{\boldsymbol{k}} \boldsymbol{\epsilon}_{\boldsymbol{k}} \sqrt{\frac{\hbar\omega_k}{\epsilon_0 V}} a_{\boldsymbol{k}} e^{i\boldsymbol{k}.\boldsymbol{r}} + \text{h.c.} \tag{3.48}$$

$$\boldsymbol{H}(\boldsymbol{r}) = \frac{1}{\mu_0} \sum_{\boldsymbol{k}} \frac{\boldsymbol{k} \times \boldsymbol{\epsilon}_{\boldsymbol{k}}}{\omega_k} \sqrt{\frac{\hbar\omega_k}{\epsilon_0 V}} a_{\boldsymbol{k}} e^{i\boldsymbol{k}.\boldsymbol{r}} + \text{h.c.} \tag{3.49}$$

Finally, one can make the transition to the continuum by taking the size of the box $L \to \infty$, so that sums like (3.49) become integrals over a continuous-valued $\boldsymbol{k}$.

Chapter 4

Quantum theory of light II

4.1 Simple features of the cavity field

Let us discuss some simple features of the electric field in a cavity. These are all properties of the harmonic oscillator you should be familiar with, so there should be no doubt about the results, even though they may seem strange in the context of electromagnetism.

Suppose we had a detector which measures the electric field associated with only a single mode i of the field. Although an idealization, this is a resonable one: real detectors respond only to a limited range of frequencies (they have a finite bandwidth) and a limited range of spatial modes (they have a finite size), so one can tailor a detector to match a given field mode. What would this detector register?

Well, suppose the mode is in an eigenstate, corresponding to a definite number of photons n. This means the radiation oscillator is in the n^{th} energy eigenstate, for which the wavefunction is

$$\begin{aligned} u_n(E_x) &= \langle E_x|n\rangle \qquad (4.1)\\ &= \frac{1}{\sqrt{2^n n!}}\left(\frac{1}{\pi\mathcal{E}_i\sin(k_i z)}\right)^{1/4} e^{-x^2/2\mathcal{E}_i^2\sin^2(k_i z)} H_n\left(\frac{E}{\mathcal{E}_i\sin(k_i z)}\right), \end{aligned}$$

where

$$H_0(x) = 1 \qquad (4.2)$$
$$H_1(x) = 2x \qquad (4.3)$$
$$H_2(x) = 4x^2 - 2 \qquad (4.4)$$
$$\ldots \qquad (4.5)$$

are Hermite polynomials. In these states our detector could measure any value of the electric field, with the probability distributions $|u_n(E_x)|^2$ shown in Fig. 4.1.

In all these states the average value of the electric field is zero, but fluctuations, measured by the standard deviation, behave as

$$\Delta E_x = \mathcal{E}_i\sin(kz)\sqrt{n+1/2}. \qquad (4.6)$$

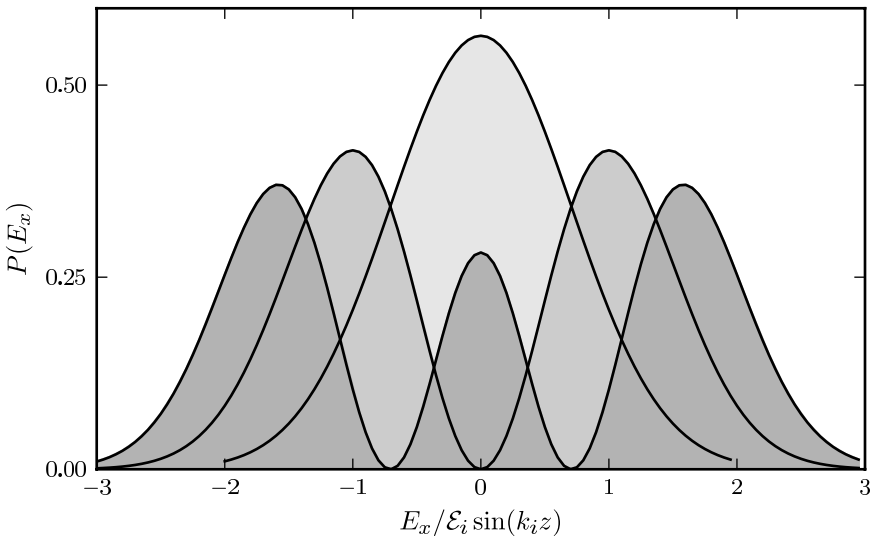

Figure 4.1: Probability distribution for a measurement of the electric field E_x in a single-mode field in the vacuum state $|0\rangle$ (lightest shading), the 1-photon number state $|1\rangle$, and the 2-photon number state $|2\rangle$ (dark shading).

In the ground state, for example, we see that although the average field is zero, typical measurements will give a modulus of the electric field $\sim \mathcal{E}_i \sin(k_i z)$. The strength of the fluctuations follows the classical mode profile $\sin(k_i z)$. And the magnitude of the fluctuations are higher for higher energy modes (larger ω_i), and if there are more photons (larger n), as perhaps one might expect. In the one-photon state for example the mean is still zero, but the we will now never measure zero electric field; instead the most likely value of the electric field is about $\mathcal{E}_i \sin(k_i z)$. This is consistent with our notion that $\mathcal{E}_i \sin(kz)$ is the electric field per photon of the mode.

We can also use our familiarity with quantum mechanics to write the uncertainty principle for the electric and magnetic field components. In particular, the statement

$$\Delta p \Delta x \geq \hbar/2 \tag{4.7}$$

translates to

$$\Delta E_x(z) \Delta B_y(z) \geq \frac{\mathcal{E}_i^2}{2c} \sin(k_i z) \cos(k_i z). \tag{4.8}$$

(These results follow from the general property $\Delta A \Delta B \geq \frac{1}{2}c$ which applies to measurements of non-commuting operators with a scalar commutator $[A, B] = c$.) The vacuum state, u_0 is one of many possible states which saturate this bound, and are referred to as a *minimum uncertainty* states. The Fock states u_n for $n \neq 0$ do not saturate this bound: the probability distribution for measurements of the field amplitudes extends over a wider range of fields than is required by the fundamental restrictions of quantum mechanics.

4.2 Multimode fields and divergent vacuum fluctuations

What happens if we allowed our detector to "see" several modes? The operators for the radiation oscillators for the different modes commute, so we could measure each component of the electric field independently. The total electric field registered by the detector is thus a sum of random variables distributed like (4.1). If all the modes are in the ground state, the total field will be Gaussian distributed with the variance $\sum_i \mathcal{E}_i^2 \sin^2(k_i z)/2$. So as we make our detector sensitive to more and more modes, we start seeing larger and larger values for the electric field – even in what we thought was the empty, lowest-energy, vacuum state. This is the "divergence of the vacuum fluctuations" in quantum electrodynamics.

It might seem strange to suggest that one can measure even a finite value of the electric field in the vacuum, let alone an arbitrarily large one. One measures a finite electric field by seeing a charge move in response to the field, in which case the field does some work on the charge. But if the field is already in its lowest-energy state there is apparently nowhere for the energy to come from.

Notwithstanding the appeal of this argument, the fluctuating electric and magnetic fields of the vacuum actually show up in experimental measurements. We shall briefly discuss one such example, the Casimir effect. A closely related effect is the Lamb shift between the $n = 2$ levels $^2S_{1/2}$ and $^2P_{1/2}$ of the hydrogen atom.

4.3 Casimir Effect

As a simple model of the Casimir effect, let us consider a square conducting box, with three sides L, L, d. The normal modes in the box have frequencies

$$\omega_{lmn} = \pi c \left(l^2/L^2 + m^2/L^2 + n^2/d^2\right)^{1/2}, \tag{4.9}$$

where the integers lmn index the modes. They range over all integer values including zero, except that no more than one of them may be zero at once. Furthermore, for modes with no zero indices there are two possible polarization states, and for modes with one zero index there is one.

Question 4.1: By writing out the electric field mode functions in the box, explain why no more than one mode index may be zero, and establish the polarization degeneracy of the modes.

Using (3.30) we can write the energy of the vacuum state of the field in the box

$$E_{\rm vac}(d) = \sum_{lmn\sigma} \frac{1}{2}\hbar\omega_{lmn}, \tag{4.10}$$

where the indices lmn label the spatial modes, and σ the polarization. Supposing that $L \gg d$, we replace the sums over l and m with integrals, to

get

$$E_{\rm vac}(d) = \frac{\hbar c L^2}{\pi^2} \sum_{n=0}^{\infty} \int dx \int dy \left(x^2 + y^2 + \pi^2 n^2/d^2\right)^{1/2} \tag{4.11}$$

$$= \frac{\hbar c L^2 \pi^2}{d^3} \sum_{n=0}^{\infty} \int_0^{\infty} dw \sqrt{w + n^2}. \tag{4.12}$$

This expression is infinite, but we are really concerned with the difference in energy from the limit $d \to \infty$, which is

$$E_{\rm vac}(d) - E_0 = \frac{\hbar c L^2 \pi^2}{d^3} \left(\sum_{n=0}^{\infty} \int_0^{\infty} dw \sqrt{w + n^2} - \int_0^{\infty} dn \int_0^{\infty} dw \sqrt{w + n^2} \right). \tag{4.13}$$

As it stands the expression in parentheses is meaningless, since we are subtracting two infinite quantities. However, recall that we are trying to describe the field in a conducting box, and conductors, or indeed any matter, becomes transparent to electromagnetic radiation at high enough frequencies. So the very high energy modes are unaffected by the confinement, and should not contribute to the difference $E_{\rm vac}(d) - E_0$. Thus we should really give the upper limits in (4.13) large finite values, related to the high-frequency cut-offs of the confinement by the box. Then we are subtracting two large finite expressions, which is certainly a legitimate thing to do. Happily, the difference comes out to be finite even in the limit where the cut-off frequencies become infinite, showing that the answer is not sensitive to the exact details of the confinement.

Since the answer does not depend on the cut-off, we are free to introduce it in any way convenient. One way is to introduce a factor $e^{-\alpha \omega_{lmn}^2}$ into the sum (4.9), and therefore a factor $e^{-z(n^2+w)}$ inside the sum and integral in (4.13). Here α and z are parameters, which model the cut-off at high frequencies, and should be taken to zero at the end of the calculation. The difference in (4.13) can then be evaluated analytically by the Euler-Maclaurin formula, or numerically, and one obtains a finite answer in the infinite cut-off limit $z \to 0$. The procedure is somewhat tedious, however, so we take it on trust that the answer is finite. In that case we can see that the answer must be

$$E_{\rm vac}(d) - E_0 = -A \frac{\hbar c L^2 \pi^2}{d^3}, \tag{4.14}$$

where A is a positive numerical factor (which actually turns out to be $1/720$). This implies that there is a force per unit area attracting the plates of

$$F = -\frac{1}{L^2} \frac{dU}{dd} = -\frac{\pi^2 \hbar c}{240} \frac{1}{d^4}. \tag{4.15}$$

This Casimir force has indeed been observed.

Chapter 5

Light-matter interactions I

In the remainder of the course, we shall look at how the electromagnetic field couples to matter, and the new effects which arise from this coupling. In this chapter we start with the simplest problem – what is the Hamiltonian describing the coupled system consisting of the electromagnetic field and a single atom? In the next lecture, we shall see the Hamiltonian for a semiconductor nanostructure, such as a quantum dot, interacting with the electromagnetic field, looks remarkably similar.

5.1 First and second quantized Hamiltonians for an atom

The Hamiltonian describing for an atom is, in the absence of an electromagnetic field,

$$\hat{H}_A = \sum_i \frac{\hat{\boldsymbol{p}}_i^2}{2m} + V_{en}(\hat{\boldsymbol{r}}_i) + \frac{1}{2}\sum_{ij} V_{ee}(\hat{\boldsymbol{r}}_i - \hat{\boldsymbol{r}}_j), \tag{5.1}$$

where the sum is over the electrons, V_{en} is the interaction energy between the electrons and the nucleus of charge $-Ze$, and V_{ee} the interaction energy (Coulomb repulsion) between the electrons. The eigenstates of this Hamiltonian form a complete set of states in the space of states of Z electrons, so in that space we have

$$\hat{1} = \sum_i |i\rangle\langle i|. \tag{5.2}$$

As eigenstates they obey

$$\hat{H}_A|i\rangle = \hbar\omega_i|i\rangle. \tag{5.3}$$

Inserting the representation of the unit operator twice, we have

$$\hat{H}_A = \sum_{ij} |i\rangle\langle i|\hat{H}|j\rangle\langle j| \tag{5.4}$$

$$= \sum_i \hbar\omega_i|i\rangle\langle i|. \tag{5.5}$$

This is a second-quantized representation for the Hamiltonian of an atom, analogous to those discussed in chapter 3 for the electromagnetic field and

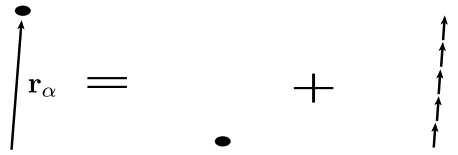

Figure 5.1: Association between a polarization distribution and a charge distribution: a charge at position $\boldsymbol{r}_\alpha$ is equivalent to a charge at the origin and a line of dipoles connecting the origin to $\boldsymbol{r}_\alpha$.

a system of electrons. It associates the energy $\hbar\omega_i$ with each eigenstate of the atom. More generally, any one-electron operator (like $\sum_i \hat{\boldsymbol{r}}_i$) for the atom can be written

$$O = \sum_{ij} |i\rangle\langle j| g_{ij}, \tag{5.6}$$

where

$$g_{ij} = \int d\boldsymbol{r} \phi^*(\boldsymbol{r}) \hat{O} \phi(\boldsymbol{r}) \tag{5.7}$$

is the matrix element of the operator $\hat{O}$. Cf. Eqs. (3.40, 3.41).

5.2 Classical light-matter interactions

The coupling between the atom and the electromagnetic field is the quantum version of the interaction energies between

- The electronic charge distribution and the electric field and
- The electronic current distribution and the magnetic field.

Suppose we have a charge q_α at a position $\boldsymbol{r}_\alpha$ close to the origin. We may express this charge distribution as a superposition of (a)a charge at the origin, and (b)a line of dipoles connecting the origin to the position $\boldsymbol{r}_\alpha$, as shown in Fig. 5.1. Thus we can associate a dipole or polarization distribution with this charge

$$\boldsymbol{P}(\boldsymbol{r}) = \lim_{n\to\infty} \sum_{p=0}^{n-1} q_\alpha \frac{\boldsymbol{r}_\alpha}{n} \delta(\boldsymbol{r} - \frac{p+0.5}{n} \boldsymbol{r}_\alpha) \tag{5.8}$$

$$= \int_0^1 du q_\alpha \boldsymbol{r}_\alpha \delta(\boldsymbol{r} - u\boldsymbol{r}_\alpha). \tag{5.9}$$

This generalizes to allow us to associate a dipole distribution with a set of charges,

$$\boldsymbol{P}(\boldsymbol{r}) = \sum_\alpha \int_0^1 du q_\alpha \boldsymbol{r}_\alpha \delta(\boldsymbol{r} - u\boldsymbol{r}_\alpha). \tag{5.10}$$

If this set of charges is neutral, $\sum_\alpha q_\alpha = 0$, the energy of the charge distribution in an electric field is

$$V_E = -\int \boldsymbol{E}(\boldsymbol{r}).\boldsymbol{P}(\boldsymbol{r}) d\boldsymbol{r}. \tag{5.11}$$

For the interaction of an atom with light, the interaction energy (5.11) can be considerably simplified, because the wavelength of light is much greater than the size of the atom (over which $\boldsymbol{P}(\boldsymbol{r})$ might be non-zero, assuming we do not ionize the atom). This fact can be used by substituting (5.10) into (5.11) and Taylor expanding the electric field near $\boldsymbol{r}_\alpha = 0$,

$$V_E = e\sum_\alpha \int_0^1 du \boldsymbol{r}_\alpha.\boldsymbol{E}(\boldsymbol{r}_\alpha u) \tag{5.12}$$

$$\approx e\sum_\alpha \int_0^1 du \boldsymbol{r}_\alpha.\left(\boldsymbol{E}(0) + u\boldsymbol{r}_\alpha.\nabla\boldsymbol{E}(0) + \ldots\right). \tag{5.13}$$

The first term in this expansion is the interaction of the atomic dipole moment with the field

$$V_{E-dip} = e\sum_\alpha \boldsymbol{r}_\alpha.\boldsymbol{E}(0), \tag{5.14}$$

the next the quadrupole interaction, and so on. We can perform a similar expansion for the magnetic energy of the currents

$$V_M = -\int \boldsymbol{B}(\boldsymbol{r}).\boldsymbol{M}(\boldsymbol{r})d\boldsymbol{r}, \tag{5.15}$$

whose leading term is the magnetic dipole energy

$$V_{M-dip} = \sum_\alpha \frac{e}{m}\boldsymbol{l}_\alpha.\boldsymbol{B}(0), \tag{5.16}$$

where $\boldsymbol{l}_\alpha = m\boldsymbol{r}_\alpha \times \dot{r}_\alpha$ is the orbital angular momentum of an electron.

Subsequent terms in the expansion (5.13) rapidly become small. If the wavelength is λ and the typical size of the atomic orbit a_B, then the second term will be smaller than the first by a factor a_B/λ. We are concerned with photons whose energy is on the order of the binding energy of the atom, of the order of the Rydberg energy, and the typical size of an atomic orbit is the Bohr radius. In this regime the ratio of the first to second term is on the order of the fine-structure constant

$$\frac{e^2}{4\pi\epsilon_0\hbar c} \approx 1/137. \tag{5.17}$$

The ratio V_{M-dip}/V_{E-dip} is also of this order. Thus, to a very good approximation, the interaction energy is just V_{E-dip}.

5.3 Quantum Hamiltonian

We can now write down the quantum Hamiltonian for an atom interacting with the electromagnetic field. It will be the sum of contributions describing the energy of the field, (3.30), the energy of the atom, (5.5), and the interaction between the two. This last is obtained by taking (5.14), and

replacing $\boldsymbol{r}_\alpha$ with a quantum-mechanical position operator, and $\boldsymbol{E}(0)$ with the electric-field operator at the position of the atom:

$$\hat{H}_c = \sum_\alpha e\hat{\boldsymbol{r}}_\alpha.\hat{\boldsymbol{E}}(0). \tag{5.18}$$

This is a one-electron operator, so we can also write it using (5.6):

$$\hat{H}_c = \sum_{ij} \boldsymbol{g}_{ij}.\hat{\boldsymbol{E}}(0), |i\rangle\langle j| \tag{5.19}$$

where $\boldsymbol{g}_{ij}$ are the matrix elements of the dipole operator $\sum_\alpha e\boldsymbol{r}_\alpha$.

5.4 Jaynes-Cummings Model

The Jaynes-Cummings model is a simple but important case, which corresponds to a two-level atom in a single-mode cavity. This applies in practice when there is a transition between the atomic ground state and an excited state whose energy is nearly equal to the energy of a cavity mode. Then we may approximate the Hamiltonian by assuming the atom is in one of these two states, and the field energy is all in this one nearly resonant mode. The resulting model is

$$\hat{H} = (\Delta/2)(|e\rangle\langle e| - |g\rangle\langle g|) + \hbar\omega\hat{a}^\dagger\hat{a} + \frac{\hbar\Omega}{2}(|e\rangle\langle g| + |g\rangle\langle e|)(\hat{a} + \hat{a}^\dagger), \tag{5.20}$$

$$= \hat{H}_A + \hat{H}_F + \hat{H}_c, \tag{5.21}$$

where Δ is the energy difference between the levels, ω the frequency of the cavity mode, $\hat{a}$ the photon annihilation operator for the cavity mode, and $\hbar\Omega$ a coupling constant which collects the numerical factors in (5.19) and (3.31). If the atom is at the antinode of the field mode illustrated in Fig.3.1 then

$$\hbar\Omega/2 = \frac{\mathcal{E}_n}{\sqrt{2}}eg, \tag{5.22}$$

where g is the matrix element of x between the atomic orbitals, and $\mathcal{E}_n$ is the field strength defined in (3.33). Notice that $\mathcal{E}_n$ increases as the volume of the mode decreases, so that the coupling between a single atom and a single photon in the mode is stronger if the cavity is smaller.

Since $\hbar\Omega \ll \Delta, \hbar\omega$, we expect to be able to solve (5.20) by treating the coupling term $\hat{H}_c$ as a perturbation. Neglecting this term, the eigenstates will just be the product of the atomic states and the Fock states,

$$|p\rangle = |e, g\rangle \otimes |n\rangle, \tag{5.23}$$

with energy

$$E_p^{(0)} = (\pm\frac{\Delta}{2}) + \hbar\omega n. \tag{5.24}$$

In general the lowest-order correction due to the coupling will be the usual second-order pertubation correction to the energy

$$\Delta E_p^{(2)} = \sum_{q\neq p} \frac{|\langle p|\hat{H}_c|q\rangle|^2}{E_p^0 - E_q^0}. \tag{5.25}$$

However, we see that if the cavity mode is close to resonance with the atomic transition then the energy differences between the states

$$|g\rangle \otimes |n\rangle \tag{5.26}$$
$$|e\rangle \otimes |n-1\rangle, \tag{5.27}$$

become very small, and the dominant contribution will come from degenerate perturbation theory rather than (5.25) (which diverges). This dominant contribution does not involve the terms

$$|e\rangle\langle g|\hat{a}^\dagger, \quad |g\rangle\langle |g\rangle\langle e|\hat{a} \tag{5.28}$$

from $\hat{H}_c$. These may therefore be dropped, an excellent approximation known as the *rotating wave approximation*. The model without these terms is called the Jaynes-Cumming model. The remaining coupling terms

$$|e\rangle\langle g|\hat{a}, \quad |g\rangle\langle e|\hat{a}^\dagger \tag{5.29}$$

correspond to processes where a photon disappears and the atom becomes excited (first term), or vice versa (second term).

5.5 Rabi splitting for one atom

The eigenstates of the Jaynes-Cummings Model

$$\hat{H} = \frac{\Delta}{2}(|e\rangle\langle e| - |g\rangle\langle g|) + \hbar\omega\hat{a}^\dagger\hat{a} + \frac{\hbar\Omega}{2}(|e\rangle\langle g|\hat{a} + \hat{a}^\dagger|g\rangle\langle e|) \tag{5.30}$$

can be found exactly. The coupling betwen the light and matter connects the states within the disconnected pairs $|g,n\rangle$ and $|e,n-1\rangle$. The eigenstates are therefore superpositions

$$|n,\pm\rangle = u_\pm|g,n\rangle + v_\pm|e,n-1\rangle, \tag{5.31}$$

(two, labelled $\pm$, for each value of the integer n). The eigenvalue equation

$$\hat{H}|n,\pm\rangle = E|n,\pm\rangle \tag{5.32}$$

gives us the energies

$$E = \hbar\omega(n-\frac{1}{2}) \pm \frac{1}{2}\sqrt{(\Delta-\hbar\omega)^2 + \hbar^2\Omega^2 n} \tag{5.33}$$

which are shown in Figs. 5.2,5.3.

Question 5.1: Show that the eigenvalues of the Jaynes-Cummings model are (5.33).

We see from Fig. 5.2 that if the energy of the atomic transition and the field mode are the same there are nonetheless two distinct eigenenergies,

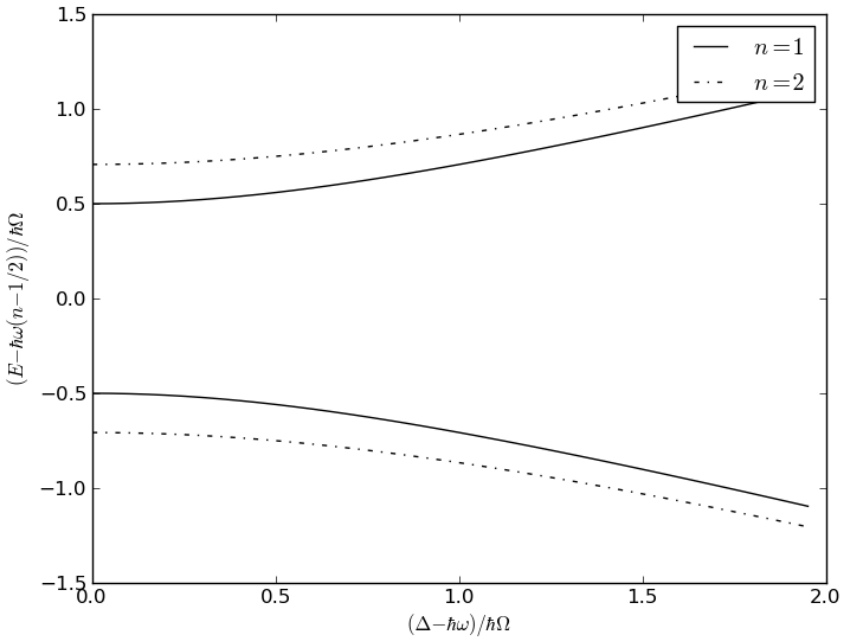

Figure 5.2: Eigenenergies of the Jaynes-Cummings model as a function of the detuning $\Delta - \hbar\omega$, for $n = 1$ (solid) and $n = 2$ (dashed).

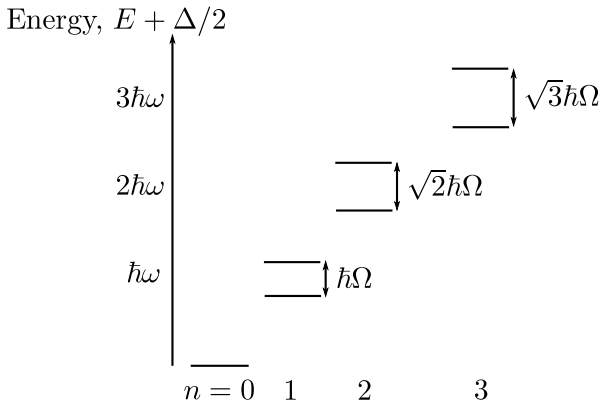

Figure 5.3: Energy levels of the Jaynes-Cummings model when $\Delta = 0$.

with a "Rabi splitting" $\hbar\Omega\sqrt{n}$. As the energies are tuned away from resonance the energy levels smoothly evolve to those of the atom and the field separately.

This Rabi splitting can be observed in various ways. The simplest is in the optical emission or absorption spectrum of the coupled cavity-atom system. Without the atom, a cavity mode absorbs a photon from outside by making the transition $|n\rangle \to |n+1\rangle$, giving a resonance in the optical response at the frequency of the mode $\hbar\omega$. This is, in quantum language, the origin of the resonances in Fig.1.2. If the cavity now contains an atom resonant with the cavity, we expect to obtain two resonances, split by an amount which depends on the number of photons in the field mode. If we start with an empty cavity mode and the atom in its ground state, and we consider the absorption of a weak probe beam, we only expect the states with $n = 0$ and $n = 1$ to be involved, so that the splitting will be $\hbar\Omega$.

An equivalent effect appears if we consider what happens when we add an atom in the excited state $|e\rangle$ to a cavity mode in its ground state. At resonance, the relevant eigenstates of the Jaynes-Cummings model are the symmetric/antisymmetric superpositions

$$|\pm\rangle = \frac{1}{\sqrt{2}}\left(|e,0\rangle \pm |g,1\rangle\right), \tag{5.34}$$

whose energies $E_\pm$ are split by $\hbar\Omega$. At $t = 0$ our state is

$$|\phi\rangle = |e,0\rangle = \frac{1}{\sqrt{2}}(|+\rangle + |-\rangle), \tag{5.35}$$

so that at time t it is

$$|\phi(t)\rangle = \frac{1}{\sqrt{2}}(e^{iE_+t/\hbar}|+\rangle + e^{iE_-t/\hbar}|-\rangle) \tag{5.36}$$

$$= e^{i(E_+ + E_-)t/\hbar}\left(\cos(\Omega t/2)|e,0\rangle + i\sin(\Omega t/2)|g,1\rangle\right). \tag{5.37}$$

Thus the probability that we observe a photon in the field is an oscillating function of the time after we added the atom. These oscillations are called vacuum Rabi oscillations. Notice that this behaviour is quite different to the familiar notion of radiative decay of an atom, where the energy is monotonically transferred from the atom to the field. This difference is because for Rabi oscillations we are concerned with coupling to a single mode of the field, whereas radiative decay arises from coupling to a continuum of modes of the field.

For Rabi oscillations to occur, the Hamiltonian must be well approximated by (5.30) for at least the Rabi period $T = 1/\Omega$. This means that the excitations of the atom and the cavity mode must have a lifetime much larger than T; in particular, we need a high-Q cavity so that the decay of the electromagnetic field can be neglected on a timescale T. The atomic excitation can also decay, in particular by emitting photons into modes other than the one cavity mode considered in (5.30).

Chapter 6

Light-matter interactions II

6.1 Review of semiconductors

Semiconductors are of course crystals, and so the basic Hamiltonian is

$$\hat{H} = \sum_i \frac{\hat{\boldsymbol{p}}_i^2}{2m} + V_{\text{lattice}}(\hat{\boldsymbol{r}}_i), \tag{6.1}$$

where $V_{lattice}$ is the periodic lattice potential, and the sum runs over the electrons. The eigenstates are the antisymmetrized wavefunctions in which the electrons occupy the Bloch orbitals of the form

$$\phi(\boldsymbol{r}) = e^{i\boldsymbol{q}.\boldsymbol{r}} u_{\boldsymbol{q},i}, \tag{6.2}$$

labelled by the Bloch wavevector $\boldsymbol{q}$ and the band index i. We shall be concerned with direct-gap semiconductors like GaAs, where the highest

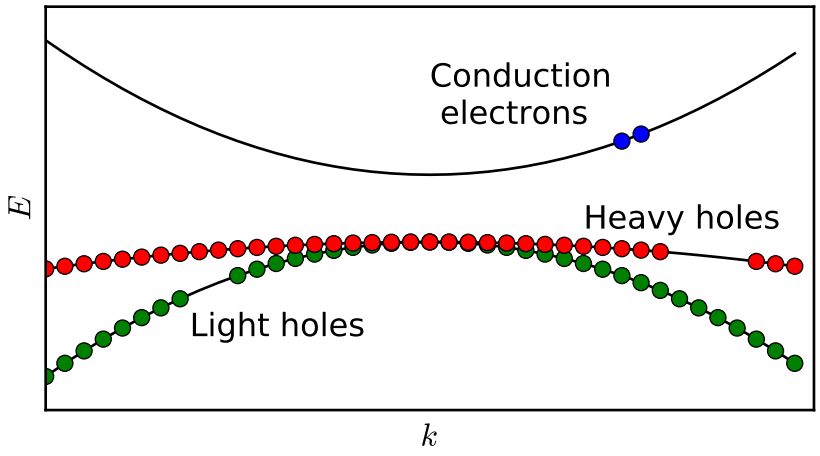

Figure 6.1: Schematic bandstructure of a zincblende semiconductor such as GaAs, with an electronic state containing electrons, heavy, and light holes.

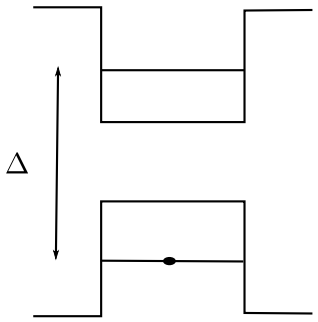

Figure 6.2: Schematic of the space-dependent band gap in a quantum well, and the localized states relevant to the optical response.

occupied orbital (HOO), and the lowest unoccupied orbital (LOO), both correspond to $q = 0$ in two different bands, called the valence and conduction bands. A simplified bandstructure for GaAs is shown in Fig. 6.1

Absorption of light for such a semiconductor, as we shall see, transfers an electron from the valence to the conduction band. The resulting state can be equivalently described in terms of a hole – an absence of an electron – in the valence band, and an electron in the conduction band.

Let us now consider what happens if we make a semiconductor inhomogeneous, that is, we send $V_{\text{lattice}} \to V_{\text{lattice}} f(\boldsymbol{r})$, where $f(r)$ is not periodic. This will modulate the bandgap, bringing the HOO and LOO together or apart with the variation in $f(\boldsymbol{r})$. If the modulation is not too strong or too rapid, then we expect the conduction-band orbital near $\boldsymbol{q} = 0$ to be of the form

$$\phi(\boldsymbol{r}) = Z(\boldsymbol{r}) u_{0,c}(\boldsymbol{r}). \tag{6.3}$$

This is called the envelope function approximation. The envelope function $Z(\boldsymbol{r})$ is determined as the eigenstate of the Hamiltonian

$$\hat{H} = \sum_i \frac{\hat{\boldsymbol{p}}_i^2}{2m_c} + V_{\text{bg}}, \tag{6.4}$$

where the lattice has disappeared into the effective potential V_{bg} and an effective mass m_c. The effective potential is the local variation in the bandgap produced by modulating the lattice potential, while the effective mass is the curvature of the band.

Quantum wells and dots are systems grown such that there is a region of space where the bandgap is reduced, so that the HOO and LOO are the localized states in the low-bandgap region, as illustrated in Fig. 6.2

The envelope function approximation can also be used to treat the effects of Coulomb interactions on the low-energy excited states consisting of an electron and a hole. These states are well approximated by the wave-

function

$$\phi(\boldsymbol{r}_e, \boldsymbol{r}_h) = Z(\boldsymbol{r}_e, \boldsymbol{r}_h) u_{0,c}(\boldsymbol{r}_e) u^*_{0,v}(\boldsymbol{r}_h), \tag{6.5}$$

where the two-particle envelope function is an eigenstate of the Hamiltonian

$$\hat{H} = \frac{\hat{p}_e^2}{2m_c} + \frac{\hat{p}_h^2}{2m_h} - \frac{e^2}{4\pi\epsilon_0\epsilon|\boldsymbol{r}_e - \boldsymbol{r}_h|}. \tag{6.6}$$

This is the same as the Hamiltonian for the hydrogen atom, so that the envelope function will be a bound state in the relative coordinate, and a plane-wave in the center-of-mass coordinate. This object is called an exciton. Adding a perturbing potential, the center-of-mass of the exciton will become localized in the regions of small bandgap.

6.2 Light-matter coupling in semiconductors

We can now see how to incorporate the effects of the electromagnetic field by analogy to the atomic case. The interaction will just be (5.19), where the states $|i\rangle$ now correspond to different configurations of the electrons among the orbitals in the crystal (rather than an atom). A standard situation is a quantum dot in a cavity, where the transition energy Δ in Fig. 6.2 is close to the energy of the cavity mode. Then the simplest approximation would be to retain only the HOO and the LOO , which are electronic states localized in the dot. We thus obtain the Jaynes-Cummings model (5.20).

Fig. 6.3 shows the experimental spectrum obtained for a single quantum dot, coupled to a single cavity mode. As expected from our discussion of the Jaynes-Cummings model, the spectrum is split by the coupling when the dot and cavity mode are resonant.

6.3 Dicke Model

The Jaynes-Cummings model applies when there is only a single relevant electronic transition – absorbing a photon onto the dot should preclude the possibility of absorbing a second. This is why, in the Jaynes-Cummings model, the Rabi splitting depends on the photon number. A much more common case involves many electronic transitions coupled to the same mode of the field. This occurs, for example, when we have a quantum well or just a bulk semiconductor embedded in a cavity – or even just light propagating in a dielectric with negligible scattering (in which case we can treat each plane-wave mode of the field separately, even without a cavity). Taking a tight-binding model of the semiconductor (or other dielectric) it is clear that the relevant model will be much like the Jaynes-Cummings model, but with many electronic transitions coupled to the field mode:

$$\begin{aligned}\hat{H} = \hbar\omega\hat{a}^\dagger\hat{a} + \sum_{i=1}^{i=N}(\Delta)|e_i\rangle\langle e_i| + \\ + \sum_{i=1}^{i=N}\frac{\hbar\Omega}{2}(|e_i\rangle\langle g|\hat{a} + \hat{a}^\dagger|g\rangle\langle e_i|).\end{aligned} \tag{6.7}$$

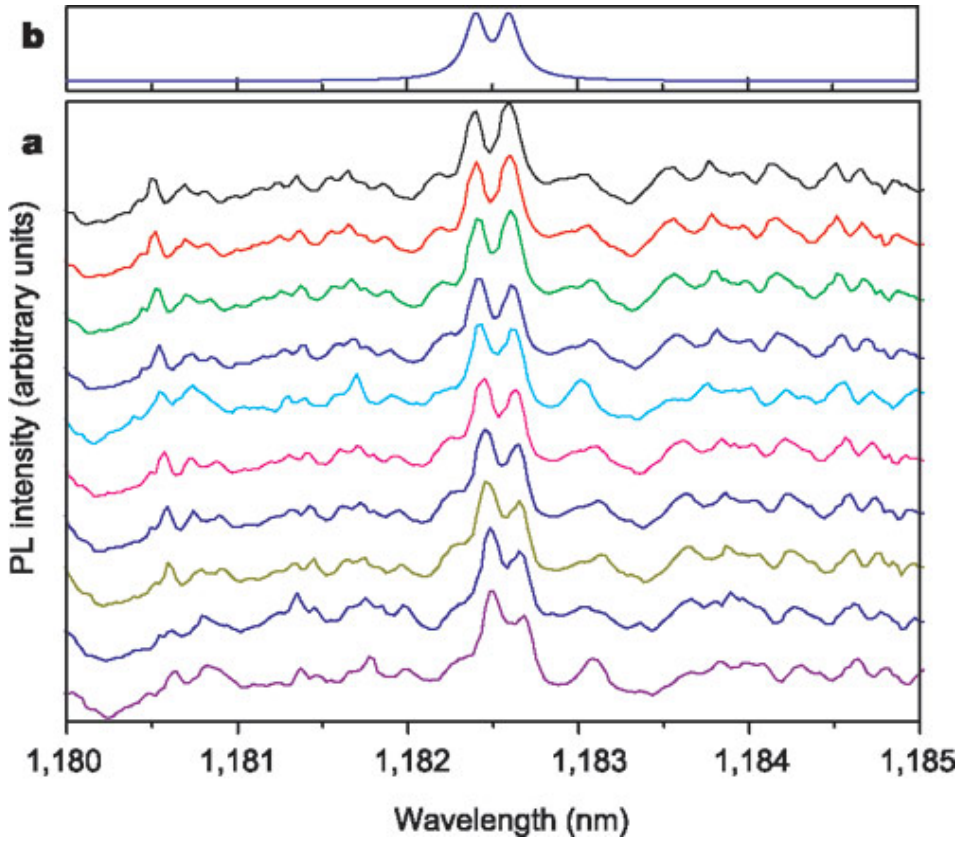

Figure 6.3: Photoluminescence spectrum. from a single quantum dot embedded in a photonic crystal microcavity, as the energy of the dot and cavity mode are scanned through one another by varying temperature [1]. Note there is always a double-peaked structure, corresponding to the splitting of the emission lines into a Rabi doublet by the coupling. Reprinted by permission from Macmillan Publishers Ltd: Nature 432, 200, copyright 2004.

This model, with N electronic transitions, is called the Dicke model. Here the state $|e_i\rangle$ denotes a state in which the i^{th} transition is excited while all the others are in their ground state

$$|e_i\rangle = |\ldots +_i \ldots\rangle, \tag{6.8}$$

and $|g\rangle$ the state where all electrons are in the ground state. We have made the rotating wave approximation discussed in chapter 5, and shifted the zero of energy so that the completely unexcited state has zero of energy.

6.4 Many-atom Rabi splitting and polaritons

The Dicke model (6.7) conserves the total number of photons and excited electrons. Let us find the eigenenergies of this model assuming that there is only one excitation. The difference between this eigenenergy and the ground state with no excitations will be the frequency at which light is

emitted from a weakly-excited system, or absorbed under weak driving. These one-excitation eigenstates must be of the form

$$|\lambda(\{c_i\}\rangle = |g,1\rangle + \sum_i c_i |e_i,0\rangle. \tag{6.9}$$

Substituting this into the eigenvalue equation we find the eigenenergies obey

$$\hbar\omega + \frac{\hbar^2\Omega^2 N}{4(E-\Delta)} = E, \tag{6.10}$$

and hence eigenenergies

$$E = \frac{1}{2}\left[(\Delta+\hbar\omega) \pm \sqrt{(\Delta-\hbar\omega)^2 + \hbar^2\Omega^2 N}\right]. \tag{6.11}$$

This spectrum is very similar to the spectrum of the Jaynes-Cummings model when $n = 1$. Similarly to (5.34), at resonance $\Delta = 0$ the coupled modes are symmetric/antisymmetric superpositions

$$|\pm\rangle = |g,1\rangle \pm \frac{1}{\sqrt{N}} \sum_i |e_i,0\rangle. \tag{6.12}$$

This sort of hybrid, light-matter state, is called a *polariton*.

One difference compared with the Jaynes-Cummings model is that the single-atom Rabi splitting $\hbar\Omega$ has become the collective Rabi splitting $\hbar\Omega\sqrt{N}$. This is just because the electric susceptibility of N transitions is N times the susceptibility of one transition (note that for a homogeneous dielectric this factor of N and the factor of V in (3.49) combine, and the splitting is finite for a macroscopic dielectric, as it must be). However, the nonlinear properties of the Dicke model are very different from those of the Jaynes-Cummings model. In particular, the spectrum of the Jaynes-Cummings model depends on the photon number on a scale of one photon, so that (say) the absorption spectrum will vary very quickly with the power. However, to make an appreciable change to the absorption spectrum of the Dicke model requires a field with of order N photons, i.e., on the order of the number of electronic transitions inside the mode volume of the field.

Question 6.1: Derive (6.10).

Question 6.2: Generalize (6.10) to include damping as a phenomenological imaginary part to the cavity mode frequency $\omega \to \omega + i\gamma$. Consider the optical spectrum at resonance $\hbar\omega = \Delta$. Plot the positions of the peaks in this optical spectrum, $\Re(E)/\hbar$ as a function of the damping term. Under what conditions is there a Rabi splitting in this damped system?

6.5 Connection to Lorenz oscillator model

The solution to the Dicke model can be understood as a quantum version of the calculation of the polariton splitting in the classical Lorenz oscillator model. In this model the electronic dipoles are assumed to behave as

damped, harmonic oscillators, driven by the applied electric field. Thus we assume a frequency-dependent relative permittivity

$$\epsilon_R(\omega) = \epsilon_R \left(1 + \frac{\Omega^2}{(\omega_0^2 - \omega^2) + i\gamma\omega}\right), \tag{6.13}$$

where Ω is an assumed parameter, related somehow to the magnitude of the induced polarization.

Let us try to calculate the resonant frequencies of an optical cavity containing a medium with permittivity (6.13). These are the (possibly complex) frequencies ω which satisfy

$$\nabla^2 E(\omega) + \omega^2 \epsilon_R(\omega) \mu E(\omega) = 0, \tag{6.14}$$

with the appropriate boundary conditions. We know that in the absence of the frequency-dependent permittivity the corresponding equation (with $\epsilon_R(\omega) = \epsilon_R$) is solved by some cavity mode frequency ω_c. Comparing the equations we have

$$\omega^2 \epsilon_R(\omega) = \omega_c^2 \epsilon_R. \tag{6.15}$$

This is a quadratic in the mode frequency ω^2; if we neglect the damping, then the result is identical to (6.10) in the close-to-resonance limit. As there, and in the Jaynes-Cummings model, away from the resonance $\omega_c \neq \omega_0$ the frequencies are basically ω_c and ω_0, but there is an "anticrossing" as the modes are tuned through one another.

6.6 Polaritons in planar cavities

We can now understand the formation of polaritons in a planar microcavity containing a quantum well [2]. In this case we have not a single cavity mode, but a continuum of modes labelled by their in-plane wavevector $\boldsymbol{k}_\parallel$; the frequency or energy of these modes disperses as shown in Fig. 2.3. However, the quantum wells have a resonant peak in their susceptibility, due to the formation of excitons. Thus if we try to tune the frequency of the cavity mode through the frequency of the exciton transition (which can be done by varying the angle), the modes will anticross, as illustrated in the Fig. 6.4. Close to the anticrossing there are two distinct peaks in the optical spectra, and the "quanta of excitation" are not excitons and photons separately, but coherent superpositions of light and matter like (6.9). Far from the anticrossing, the excitations are essentially excitons or photons, and only the latter gives a strong peak in the optical spectra.

6.7 Bibliography

[1] T. Yoshie, A. Scherer, J. Hendrickson, G. Khitrova, H. M. Gibbs, G. Rupper, C. Ell, O. B. Shchekin, and D. G. Deppe, Nature **432**, 200 (2004), ISSN 0028-0836, DOI: 10.1038/nature03119.

[2] C. Weisbuch, M. Nishioka, A. Ishikawa, and Y. Arakawa, Phys. Rev. Lett. **69**, 3314 (1992).

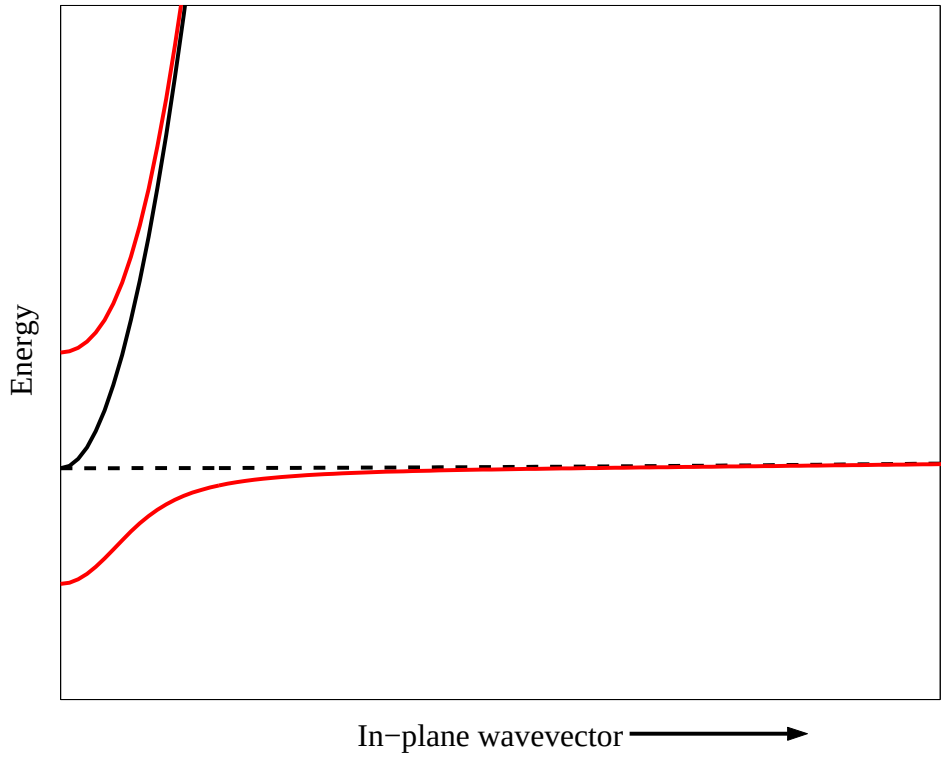

Figure 6.4: Schematic of the excitation energies (red) as a function of in-plane wavevector for a microcavity containing quantum wells. The dotted line is the exciton energy in the quantum well, and the solid black line the energy of the cavity mode.